ELECTRODEPOSITION OF NICKEL-METALLOID ALLOY FILMS AND THEIR INVESTIGATION FOR ELECTROCATALYTIC WATER SPLITTING

SSEMWANGA HERBERT

(BST/C)

18/U/GMCH/19521/PD

A DISSERTATION SUBMITED TO THE GRADUATE SCHOOL IN PARTIAL FULFILLINMENT OF THE REQUIREMENTS FOR THE AWARD OF A MASTER OF SCIENCE IN CHEMISTRY DEGREE OF KYAMBOGO UNIVERSITY

MARCH 2021

DECLARATION

I Ssemwanga Herbert (Reg. No. 18/U/GMCH/19521/PD) declare that this dissertation presented for the award of a Master of Science degree in Chemistry has not been wholly or partially submitted to any institution for any degree award or professional qualification.

Signed…… Date……...

APPROVAL

This is to certify that Ssemwanga Herbert carried out this research work titled “Electrodeposition of nickel-metalloid alloy films and their investigation for electrocatalytic water splitting” under our supervision.

1) **Dr. Justus Masa**

   Senior Lecturer,

   Department of Chemistry,

   Faculty of Science,

   Kyambogo University

   Signature ……... Date……

2) **Dr. William Wanasolo**

   Senior Lecturer,

   Department of Chemistry,

   Faculty of Science,

   Kyambogo University

   Signature……... Date……

DEDICATION

I dedicate this dissertation to the memory of my grandmother and guardian of all times, the late Jajja Alice Nanyunja Muleto. She greatly supported my education. May her soul rest in eternal peace.

Also to my dear mother, the late Goreth Namutebi and my dear father, the late Sunday Stanley Musisi. May their souls rest in eternal peace.

ACKNOWLEDGEMENT

I thank the Almighty God for the gift of life and an opportunity to complete this study.

I acknowledge with thanks my supervisors for their special contribution which has resulted in this dissertation. I thus sincerely thank my supervisors Dr. Justus Masa and Dr. William Wanasolo for their continuous and tireless efforts to provide guidance throughout this study. May God greatly reward them.

I am highly indebted to Dr. Justus Masa for his kind personal contribution to this exciting research project by providing me with the equipment and all materials needed. This has therefore enabled me to complete the first masters electrochemistry project in Kyambogo University. I will forever remain grateful for this support. May God richly bless him.

Furthermore, I would like to thank Mr. John Opendun for giving a helping hand during my laboratory sessions and may God richly bless him. Mr. Richard Namakajjo of Uganda National Bureau of standards for his guidance and encouragement during this project.

Special thanks go to my workmates at Uganda Industrial Research Institute like; Prof. Vinand Nantulya, Dr. George Mukibi- Muka, Mrs. Namirembe Rose Jackie Bukenya, Ms. Bridgette Ntale, Mrs. Judith Chemos, Mr. Brian Bigirwa, Ms. Sylvia Muwanika, Mr. Okello Boniface, Mrs. Emma Mbabazi, Ms. Adrine Atukwatse and last but not least Mr. Namawa Godfrey for providing an enabling environment during this study.

Finally, I would like to thank my fiancé Ms. Christine Nabagereka Ssemwanga and my sons; Hilton Ssemwanga, Herman Ssemwanga, Stanley Ssemwanga and Harry Ssemwanga who have collectively encouraged me and supported me morally and emotionally while undertaking this study and throughout the entire master's program.

TABLE OF CONTENTS

LIST OF FIGURES

LIST OF TABLES

LIST OF ABBREVIATIONS

ALKWE	Alkaline Water Electrolysis
CHI	Electrochemical Instrumentation
CV	Cyclic Voltammetry
GC	Glassy Carbon
HER	Hydrogen Evolution Reaction
LSV	Linear Sweep Voltammetry
NiB	Nickel Boride
NiP	Nickel Phosphide
NiTe	Nickel Telluride
OER	Oxygen Evolution Reaction
PEM	Polymer Electrolyte Membrane
PtX	Power- to – X
RHE	Reversible Hydrogen Electrode
SOEC	Solid Oxide Electrolysis

ABSTRACT

Electrocatalytic splitting of the water molecule to produce hydrogen as an energy carrier provides a very promising pathway for provision of green and inexhaustible renewable energy for the future. The bottleneck of this reaction is the sluggish kinetics of the OER that makes the processes to be extremely energy intensive. Electrochemists have devoted much research efforts in finding cost-effective electrocatalysts that can speed up the OER during electrochemical water splitting. In this study, reference (NiB, NiP and NiTe) metalloid alloy powders pre-synthesized at Ruhr University, Germany and (Ni-Ga and Ni-In) metalloid films synthesized by electrodeposition were investigated for the OER activity in an alkaline electrolyte using LSV. The results showed that the optimal number of CV deposition cycles for the highest OER activity were 7 for Ni, 7 for Ga,3 for In,7 for Ni-In and 5 for Ni-Ga composite electrocatalytic films. The OER activity of $Ni(OH)_2$ formed by electrodeposition was several fold higher than that of the pure Ga and In films, as well as of the composite Ni-Ga and Ni-In films. It was concluded that CV deposition cycles that had the highest activity and therefore the highest performance were; 7 for Ni, 7 for Ga ,3 for In ,7 for Ni-In and 5 for Ni-Ga composite electrocatalytic films respectively. Ga and In species exist as discrete domains rather than alloys in the Ni-Ga and Ni-In composite films. The attempted method for synthesis of Ni-Ga and Ni-In alloy films by electrodeposition most likely led to the formation of Ni-Ga and Ni-In composite films with discrete domains of oxides of their respective elements but not alloys.

CHAPTER ONE

INTRODUCTION

1.1 . Background

There is growing demand for energy globally due to population growth and industrialization. Over the years, fossil fuels have been used to drive society in the form of transportation networks and technology. Fossil fuels are mostly in the form of crude oil, coal and natural gas. Continuing to use fossil fuels puts life at risk due to pollution and global warming that is associated with their use (Crabtree *et al*., 2004a), in addition to the risk of their imminent eventual total depletion.

Hydrogen is a promising alternative to fossil fuels. Hydrogen reacts explosively with oxygen in heat engines or quietly in fuels cells to release energy with water produced as its only by-product. Although hydrogen does not occur freely in nature, it is abundantly distributed globally in chemical compounds like water and hydrocarbons from which it can be obtained. Using hydrogen to create a future energy system based on hydrogen and electricity, the hydrogen economy, would produce a clean energy resource with global accessibility (Guy, 2000). The Hydrogen economy is a concept where the future energy infrastructure including electricity is primarily based on hydrogen (Bockris, 1972).

Currently most of the hydrogen available on the market is produced by steam methane reforming which is linked to fossil fuels. There is need to produce hydrogen from renewable resources such as water so as to fully benefit from a truly green hydrogen economy. The available technical means of hydrogen production, storage and use cannot yet compete with fossil fuels in terms of reliability, cost and performance (Fabbri et al., 2014a) .

The most promising route of producing hydrogen from renewable resources is through water splitting. Water is a very stable compound which requires energy to split into hydrogen and oxygen. The energy used in water splitting must come from a renewable energy source like wind and solar in order to make the process sustainable and environmentally friendly (You & Sun, 2018).

In the natural world, the hydrogen economy includes plants using photosynthesis to convert water, sunlight and carbon dioxide into carbohydrates and oxygen. The hydrogen in water is used by the plants to manufacture carbohydrates while the oxygen is emitted in the atmosphere where it is used by animals during respiration. Plants use a manganese-oxide based catalyst to evolve oxygen from water at room temperature while bacteria use iron and nickel clusters to produce hydrogen from water (Marbán & Valdés-Solís, 2007). The natural processes of water splitting provide insights for research on the most cost effective methods for water splitting to produce hydrogen and oxygen using artificial materials (Crabtree *et al*., 2004a). The schematic depiction of hydrogen production in the coming energy revolution (the hydrogen economy) is as shown in Figure 1 .

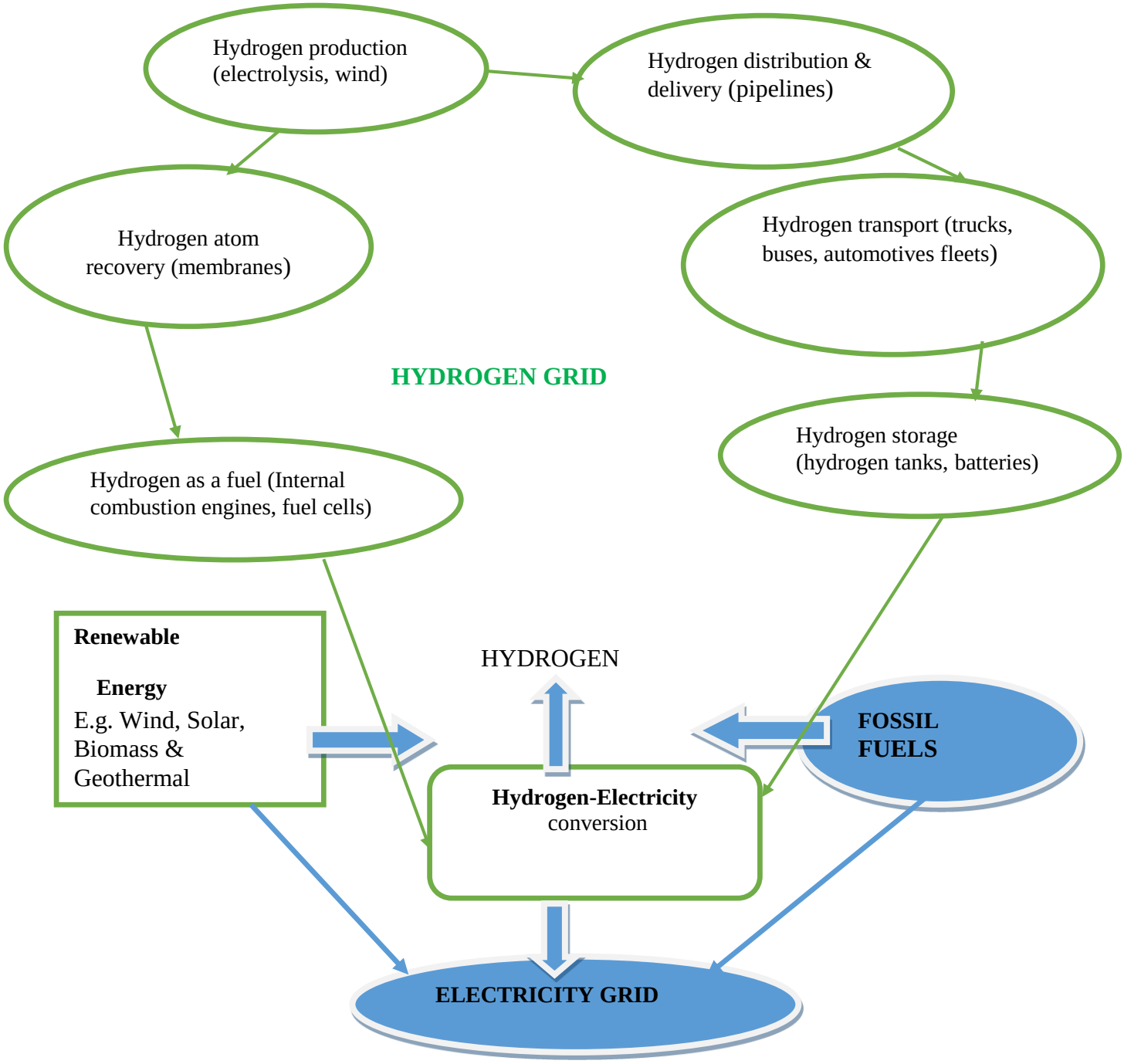

Figure 1: *A schematic integration depicting production of hydrogen in the coming energy revolution (The hydrogen economy – a concept in which the future energy infrastructure including electricity will be primarily based on Hydrogen). Adopted with modifications from (Armor, 2005).*

1.1.1. Electrocatalytic water splitting

Electrolysis of water is the most promising clean technology for hydrogen production with a high purity of more than 99 % (McCrory *et al*., 2013). The present production systems use expensive and scarce platinum group metal electrocatalysts which makes up for a significant part of the total production cost. Recent research efforts have been devoted to producing low cost effective electrocatalysts for producing hydrogen via cathodic hydrogen evolution reaction (HER) and producing oxygen via anodic oxygen evolution reaction (OER)(J. Li *et al.*, 2016). A number of nickel based materials over the years have been developed as earth abundant low cost non noble metal heterogeneous electro-catalysts for OER (Suen et al., 2017). These bring down the activation energy or the over potential of the electrocatalytic water splitting and thus the total production cost of hydrogen. There are three main water electrolysis technologies used for hydrogen production classified according to the type of electrolyte used. These are: alkaline water electrolysis (ALKWE)(Ni *et al*., 2007), polymer electrolyte membrane electrolysis (PEM)(Millet et al., 2011a) and solid oxide electrolysis (SOEC)(Roger *et al*., 2017).

The ALKWE is a developed technology with large-scale commercial hydrogen production systems. The problems associated with ALKWE are; low current density, poor system stability mainly due to corrosion of the catalyst (Daly & Barry, 2003). The PEM systems are mainly used for small scale production of hydrogen. The problems associated with PEM are fast degradation of membranes and high cost due to the exclusive use of platinum group metals as catalysts. The SOEC is still at the stage of prototypes and the problems associated with it include low cell stability and it's not suited for fluctuating systems (de Vasconcelos & Lavoie, 2019). A schematic drawing showing the typical features of electrocatalytic water splitting in an electrochemical cell is as shown in Figure 2.

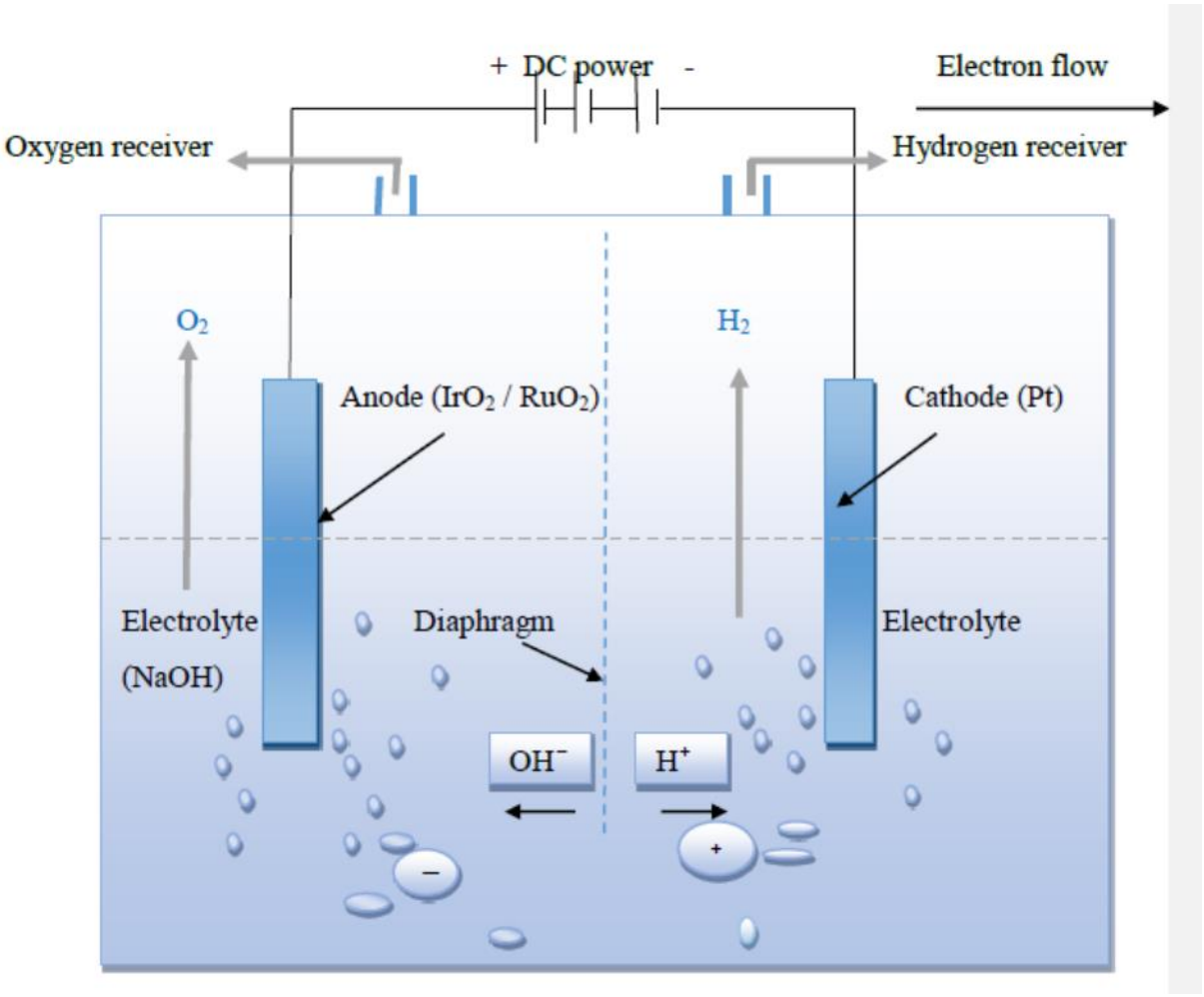

Figure 2: *Typical features of electrocatalytic water splitting in an alkaline electrochemical cell in which 1M NaOH is used as the electrolyte at room temperature. Electrons flow from the anode to the cathode where they are consumed by protons to produce Hydrogen while oxygen is evolved at the anode. Adopted with modifications from (Zeng & Zhang, 2010).*

1.1.2. Metal and metal oxide electrodeposition

Electrodeposition is a well-known method used to produce in situ metallic coatings by the action of an electric current on a conductive material immersed in a solution containing a salt of the metal

to be deposited (Garcia *et al*., 2013). Electrodeposition of metal or metal oxides is one of the oldest themes in electrochemical science and it remains a much-studied subject. It is mainly applied in the fabrication of electrodes for supercapacitors and other electrochemical cell devices like solar cells (Walter et al., 2010). The electrodeposition of nickel oxides, copper oxides, titanium oxides to form films for heterogeneous catalysis and others is a very active research area because of high efficiency and the low cost of the electrochemical method (Ngamlerdpokin & Tantavichet, 2014). Electrodeposition is used in forming protective coating on electrical interconnects in solid oxide fuel cells (SOFC) (Yu *et al*., 2018).

1.1.3. Nickle metalloid-alloys as water splitting electrocatalysts.

A metalloid has properties that are intermediate between those of metals and non-metals. Alloys are made by melting two or more elements together, at least one of them being a metal (Fu et al., 2009; Gangasingh & Talbot, 1991).

In this case the nickel-metalloid alloys of boron, silicon, arsenic, phosphorus and tellurium are considered as highly promising water oxidation electro-catalysts (Masa *et al*., 2019). Currently the production of hydrogen by water electrolysis is based on expensive and rare electrocatalysts like platinum at the cathode for the hydrogen evolution reaction (HER) while at the anode noble metal oxides like ruthenium oxide (RuO_2) and iridium oxide (IrO_2) are used for the oxygen evolution reaction (OER) (McCrory *et al*., 2013). The prices of the metals used for making electrocatalyst for water splitting are as shown in Table 1.

Table 1 : Price of Metals used for making electrocatalysts for Water splitting (*Daily Metal Price: Ruthenium Price (USD / Kilogram) for the Last Day*, January 25,2021).

METAL	PRICE / Kg (USD)
Ir	125,387
Ru	10,288
Pt	34,980
Ni	17.73

There is a need to devote more research efforts to fully understand the chemistry of nickel metalloid-alloys as an emerging class of low cost electrocatalysts with a potential to replace the platinum group elements in OER and HER catalysis (Masa *et al*., 2019).

The kinetic bottleneck in the electrocatalytic water splitting is the OER. This is because the OER half-reaction requires a higher overpotential above the theoretical equilibrium potential of 1.23 V to deliver the same current as the HER (J. Li et al., 2016). This is graphically shown in Figure 3.

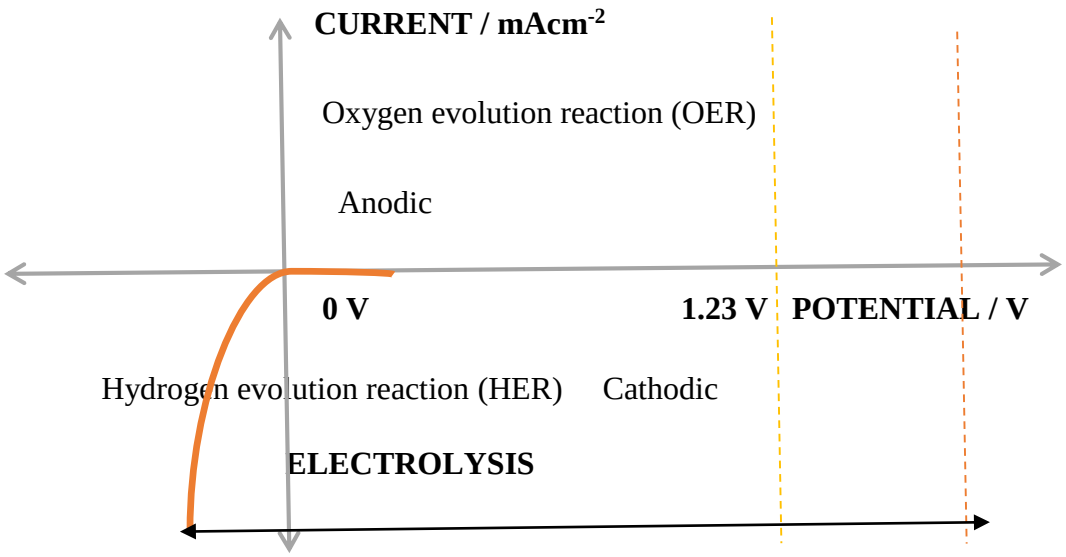

Figure 3: *A graphical representation of the HER and OER in electrocatalytic water splitting.*

1.2. Problem statement

The continued use of fossil fuels as a source of energy has put life at risk. This is due to the pollution and the global warming associated with use of fossil fuels like petroleum, coal and natural gas (Bockris, 1972). There is therefore an urgent need to find green and renewable energy alternatives. Hydrogen is one such promising fuel alternative (Crabtree *et al*., 2004b). However, hydrogen does not occur freely in nature. Currently hydrogen is produced by steam reforming of methane. This method however denies the hydrogen economy of its very much needed positive benefits. Literature has shown that through electrolysis, water can be split to generate hydrogen which is a clean and renewable source of energy (McCrory et al., 2015) . Water is a very stable molecule and so splitting it into hydrogen and oxygen requires a high activation energy. Electrocatalysts are used to lower the activation energy required. The main challenge is that expensive (precious metals) as shown in Table 1 have to be used at both the anode (iridium oxide, ruthenium oxide or their mixture) and cathode (platinum usually). These metals are not only very expensive but also very scarce. This makes the production of hydrogen very expensive and thus limiting its wide commercial production. The goal of this research was to develop low-cost materials that can potentially substitute these precious and rare metals in electrocatalytic water splitting. For this case, pre-synthesized nickel-metalloid (B, P, Te) alloy powders used as reference materials and nickel-metalloid (Ga, In) alloy films prepared by electrodeposition were investigated as potential alternatives to replace the precious and rare metals in water electrolysis. The developed nickel-metalloid films were tested for their activity as electrocatalysts for the oxygen evolution reaction in electrochemical water splitting.

1.3. Objectives

1.3.1. General objective

To electrodeposition nickel metalloid (In, Ga) alloy films and investigate their oxygen evolution reaction (OER) activity in electrocatalytic water splitting.

1.3.2. Specific objectives

1) To prepare Ni-In and Ni-Ga metalloid alloy films by electrochemical deposition.
2) To determine the oxygen evolution reaction (OER) activity of electrodeposited Ni-In and Ni-Ga films in electrocatalytic water splitting.

1.4. Scope

The scope of this study is limited to pre-synthesized nickel metalloid (B, P, Te) alloy powders used as reference materials and nickel metalloid (In, Ga) alloy films prepared by electrodeposition using cyclic voltammetry to their investigation for the oxygen evolution reaction in a 1.0 M NaOH electrolyte using linear sweep voltammetry. This was done from May 2019 to March 2020 at the chemistry research laboratory of Kyambogo university, Kampala Uganda.

1.5. Hypotheses

In this study, the following hypotheses were used;

1. For Ni-Ga and Ni-In metalloid alloy electrocatalytic films prepared by electrodeposition, there exists an optimal number of electrodeposition cycles for the highest OER activity because the number of deposition cycles is one of the factors that determine the activity of the electrodeposited electrocatalytic film.

2. The nickel-gallium and nickel-indium films prepared by electrodeposition would have a better electrocatalytic OER activity than pure nickel films in alkaline electrolyte at room temperature because the guest metalloid element (Gallium / Indium) in the respective alloy formed enhances the electrocatalytic activity of nickel.

1.6 . Justification

Electrocatalytic splitting of water to produce hydrogen at the cathode and oxygen at the anode in an electrolyzer provides a potentially carbon-neutral alternative route for hydrogen production if the energy used to power the electrolyzer is renewable or from a carbon-free source, such as nuclear energy (Zeng & Zhang, 2010). The main challenge is that expensive (precious noble metals) have to be used at both the anode (iridium oxide, ruthenium oxide or their mixture) and cathode (platinum usually)(Masa & Schuhmann, 2019). These metals are not only very expensive but also very scarce. The kinetic bottleneck of the electrocatalytic water splitting however is the oxygen evolution reaction (OER). There is a need to develop low-cost OER electrocatalysts that can substitute these precious and rare metals. For this case, pre-synthesized nickel-metalloid alloys, and nickel-metalloid alloys prepared by electrodeposition method were investigated as potential candidates to replace the precious metals as OER electrocatalysts in water electrolysis (Masa *et al*., 2019).

1.7. Significance

This study will provide information and data to the Government of Uganda on hydrogen as a renewable energy source which will promote its sustainable development and utilization (Development, 2019). It will also provide information to researchers and electrochemists in the field of electrocatalysis and renewable energy that will be used for benchmarking and developing low-cost materials (nickel metalloid alloys) as potential electrocatalysts that can substitute

precious and rare metals for electrochemical production of hydrogen in electrocatalytic water splitting. This will further enable research and development efforts in deeper understanding of the chemistry, preparation techniques and material design of oxygen evolution reaction catalysts in alkaline electrolytes and thus facilitate their further improvement towards widespread commercialization of hydrogen production from electrochemical water splitting.

CHAPTER TWO

LITERATURE REVIEW

2.1. Background

Continuing depletion of fossil fuels plus the climate and health hazards associated with them, have inspired the current search for clean and renewable fuel alternatives like hydrogen. For around 200 years, production of Hydrogen by electrolysis of water has been known. However only 4% of the world's hydrogen is produced by electrolysis of water (Zeng & Zhang, 2010). Most of the hydrogen is currently produced by steam reforming of methane and coal gasification.

This is due to the use of rare and expensive platinum group metals in electrocatalytic water splitting. There is thus an urgent need to search for cheap and earth abundant electrocatalysts which are durable and of high catalytic activity (Fabbri et al., 2014a; Masa & Schuhmann, 2019).

Electrodeposition of nickel has been studied since the beginning of the 20th century (Andricacos et al., 1989) . Over the last 20 years there has been an increased interest and it is now one of the most frequently used methods for surface treatments (Oriňáková et al., 2006). Saitou et al described the growth of the nickel film prepared by electrodeposition. Nickel alloys with other metals and materials have significantly contributed to our present-day society and even continue to provide materials for a more demanding future. In the industry now more than 200 binary alloys are used. Electrodeposition of films can be controlled easily, takes place at room temperature and pressure and uses relatively cheap and economically modest equipment.

2.2. The hydrogen economy

Technologies and transportation networks that drive society have been in existence since the industrial revolution and powered by fossil fuels. Due to population growth and industrialization of developing countries, in 2004 the US department of energy projected the world energy demand to double by 2050. The use of fossil fuels has contributed greatly to environmental pollution and global warming. Hence there is a need to change to renewable and green energy resources like wind and solar to abate environmental pollution and prevent the potential catastrophic consequences of climate change and global warming (Crabtree et al., 2004a).

Extensive research and development of new energy technologies, designs and materials are however much needed to manage the energy transition. The alternatives should favorably compete with fossil fuels regarding quality, quantity and cost (Fabbri et al., 2014b). This implies that research into new alternative fuel sources is necessary.

Hydrogen is a very promising fuel alternative, not only because it is inexhaustibly abundant and omnipresent but water is the only by-product when hydrogen is used as a fuel. It is only scientific and technological developments that are required to create a robust hydrogen economy of global significance. Functional steps in the hydrogen economy are; production, storage and use (Crabtree *et al.*, 2004a).

Hydrogen does not exist freely in nature. Commercially, hydrogen is currently produced by steam reforming of methane which undermines the hydrogen economy of its much aspired environmental benefits. For the hydrogen economy to deliver its promise, hydrogen must be produced from clean, renewable sources. Electrocatalytic splitting of water provides the most suitable alternative for hydrogen production (Suen et al., 2017; Tahir et al., 2017). This involves the cathodic hydrogen

evolution reaction and the anodic oxygen evolution reaction. Electrocatalysts are necessary to lower the reaction overpotential since water is a very stable molecule (Walter et al., 2010).

Expensive and rare catalysts are currently used in water electrolysis, that is, platinum for the cathode and noble metal oxides (IrO_2 and RuO_2) at the anode thus limiting the commercial viability of hydrogen production through water splitting.

2.3. Power – to - x (PtX) technology for the production of fuels and chemicals.

Renewable energies such as wind power and solar are playing a key role in the transition from fossil fuels to clean, emission free fuels. For a successful transition, focus should be put on renewable energy storage issues. Power- to – x (PtX) technologies convert renewable electricity to chemicals and fuels that are transported and stored more easily. Water electrolysis produces hydrogen which can be used directly in fuel cells or used to reduce carbon dioxide into chemicals and fuels that can be easily transported with the existing infrastructure (Arunachalam & Al Mayouf, 2018).

The electroreduction of carbon dioxide on copper catalyst in an electrolysis cell into methane (equation 1), ethylene (equation 2), formate (equation 3) and methanol (equation 4) at pH 6.8 when a standard reduction potential is applied was reported in literature by (Kuhl *et al*., 2012).

$$CO_2 + 8e^- \xrightarrow{E=0.17\,V,\ Cu,\ pH\ 6.8} CH_4 \quad (Methane) \text{ .....} \textbf{\textit{Equation(1)}}$$

$$CO_2 + 12e^- \xrightarrow{E=0.08\,V,Cu,\ pH\ 6.8} C = C \ (Ethylene) \text{ .....} \textbf{\textit{Equation(2)}}$$

$$CO_2 + 2e^- \xrightarrow{E=-0.02\,V,\ Cu,\ pH\ 6.8} CHOO^- \ (Formate) \text{.....} \textbf{\textit{Equation(3)}}$$

$$CO_2 + 6e^- \xrightarrow{E=0.03V,\ Cu,\ pH\ 6.8} CH_3OH \ (Methanol) \text{ .....} \textbf{\textit{Equation (4)}}$$

Using renewable electricity, carbon dioxide is directly converted to value –added products by its electrochemical reduction. Recent PtX technologies include the production of key chemicals like methane (equation 1), methanol (equation 4), formic acid and formaldehyde (equation 3) and fuels like jet fuel and diesel (de Vasconcelos & Lavoie, 2019). This implies that with more research efforts useful products can be obtained from the otherwise pollutant greenhouse gases like carbon dioxide.

There is a growing need to reduce greenhouse gas emission globally and switch to clean renewable energies. The demand for energy (a fundamental survival requirement) is ever growing as a significant portion of the world population reaches the middle class.

There is a gigantic demand for transportation fuels around the world. Some of the options include using electric vehicles in countries where green electricity is abundant and production of biofuels from renewable carbon sources or biofuels.

The transitioning from fossil fuels to renewable energies has got some enormous challenges like the alternating flux of the produced electricity. There is optimal production during some peak periods which doesn't most of the time fit to the demands. It's risky to rely on these sole options especially for use in large cities. This has over the years become a significant concern for industry and governments and a major research challenge in academia. Applications for hydrogen include; fine chemicals, metallurgy, aerospace industry and hydrogen filling stations (Niaz et al., 2015).

Other PtX technologies include; carbon dioxide derived chemicals from CO_2 electrochemical reduction (e.g. formic acid, methanol, and ethanol) and CO_2 hydrogenation. PtX technologies have thus gained considerable attention since it produces carbon neutral fuels from CO_2 as a means for storage of renewable energy (Marbán & Valdés-Solís, 2007).

Current PtX technologies thus mainly focus on two processes, namely, hydrogen production by water electrolysis using renewable energy and CO_2 conversion to chemicals and fuels.

2.4. Alkaline water electrolysis (ALKWE)

In alkaline water electrolysis two electrodes immersed in a strong alkaline liquid electrolyte (KOH or NaOH) are used. To avoid the product gases (oxygen and hydrogen) from mixing, a diaphragm made of Nafion is used to separate the electrodes. Despite electrolytic water splitting being faster in acidic electrolytes, alkaline water electrolysis is presently the most used technology in commercial hydrogen production due to the possibility to use low-cost nickel based electrodes as opposed to acidic water splitting that requires the use of precious metals (Seitz et al., 2016; You & Sun, 2018). Maintenance, cost and energy requirements must be reduced in addition to increasing safety, reliability and durability so as to ensure widespread use of water electrolysis(Maeda & Domen, 2010). This implies that more research and development is required to design electrocatalysts that lower the overpotential in electrocatalytic water splitting and thus bring down the production costs (Daly & Barry, 2003).

There are three categories of resistance in water electrolyzers that contribute to high reaction overpotential, namely; transport resistance, reaction resistance and electrical resistance. By means of thermodynamics and kinetics, each of these resistances is studied to provide insights on achieving greater efficiency in alkaline water electrolysis. The dependence of the overall reaction kinetics on resistances to ion transfer, alkaline concentration and electrode surface reaction sites is revealed through kinetic analysis (Millet et al., 2011b).

Water electrolysis produces highly pure hydrogen. However, presently its application is limited to small scale uses and where access to large scale hydrogen plants is not economical or possible, for

example, in the food industry, medical applications, electronics industry, rockets, marine and space crafts. Only 4% of the world hydrogen production is produced by water electrolysis.

Hydrogen is increasingly becoming the clean renewable energy source of choice. This is because it produces water as its only byproduct, it can be produced using green renewable energy sources like wind and solar, it works with fuel cells and together they can solve the supply and demand puzzle in the hydrogen economy. With abundant supply of renewable energy, excessive energy can be stored in the form of hydrogen by water electrolysis. This can be later used to generate electricity in fuel cells or it can be used as fuel gas (Zeng & Zhang, 2010). This implies that with more research and improvements, hydrogen as a fuel has got great chances to replace fossil fuels. Hydrogen produced from renewable energy sources has the great advantage of portability which is essential for use in remote locations away from the main electricity grid. Hydrogen and oxygen produced from water electrolysis can be used to replace oxygen- acetylene for metal cutting, braising and welding. Pure oxygen, a co-product of hydrogen generation, produced on a small scale can be used in laboratories and in hospitals to provide life support.

The advantages of hydrogen production from water electrolysis include; wide spread applications, availability, high purity and flexibility. Various improvements are however still needed in terms of portability, safety, durability, energy efficiency, operability, storage and reduction in operation and installation costs. The opportunities for research and development for technological advancement in water electrolysis are thus enormous (Andricacos et al., 1989; Fu et al., 2009).

An alkaline water electrolyser has an anode, cathode, electrolyte and power supply. Electrons flow from the anode to the cathode where they are consumed by protons to produce hydrogen and OH^-according to equation (5) while oxygen is produced at the anode according to equation (6), the overall cell reaction is as shown in equation (7).

$$2\,H_2O(l) + 2\,e^- \rightarrow H_2(g) + 2\,OH^-(aq) \ldots\ldots\ldots\ldots\ldots \textbf{\textit{Equation (5)}}$$

$$4\,OH^-(aq) \rightarrow O_2(g) + 2\,H_2O\,(l) + 4\,e^- \ldots\ldots\ldots\ldots\ldots\ldots \textbf{\textit{Equation (6)}}$$

$$2\,H_2O\,(l) \rightarrow 2\,H_2(g) + O_2(g) \ldots\ldots\ldots\ldots\ldots\ldots\ldots\ldots \textbf{\textit{Equation (7)}}$$

Hydrogen production by alkaline water electrolysis is simple but still inefficient. Efficiency, safety and durability are still its main limiting factors. Further research and development efforts are therefore required to overcome these challenges. The research efforts should mainly focus on the following: reducing electrochemical reaction resistance by developing more efficient electrocatalysts that facilitate fast electron transfer, fast ionic transfer through electrolyte additives, and managing bubble resistances through electrode surface modifications and coatings (Tahir et al., 2017; Walter et al., 2010).

2.5. Polymer electrolyte membrane (PEM) water electrolysis.

Polymer electrolyte membrane or proton exchange membrane (PEM) electrolysis is a commercially viable technology for hydrogen production. High quality hydrogen (≈ 100%) can be produced by catalytic splitting of water to produce hydrogen and oxygen (Tee et al., 2017). Despite many years of research on PEM water electrolysis, there are still many unresolved challenges that prevent its wide scale use (Carmo *et al*., 2013). This implies that further research in this area is inevitable.

Some of the advantages of PEM electrolysis include; high current densities, high voltage efficiency, good partial load range, rapid system response, high gas purity, dynamic operation and compact system design. Low gas crossover, high proton conductivity, compact system design and high pressure operation are all due to the polymer electrolyte membrane with a low thickness in the range of 20 to 300 µm (Millet et al., 2011b).

PEM electrolysis has got disadvantages like; high cost of components, acidic corrosive environment and poor durability that inhibit its wider commercialization. Significant breakthroughs in this regard require intensive research and development efforts including: enhancing long-term durability, reduction or substitution of noble metal catalysts, reduction in costs of current collectors and separator plates, development of microporous layers, and improvement of membrane characteristics (conductivity and mechanical strength) (Carmo *et al*., 2013). Future research on PEM electrolysis should thus aim at developing cost effective and reliable PEM electrolysers so as to contribute to the development of the hydrogen economy.

2.6. Electrocatalysts for water electrolysis.

Less than 4% of the world's commercial hydrogen is produced by water electrolysis. This is due to the scarcity and high cost of the traditional noble metal catalysts like platinum, ruthenium and iridium metals used in acidic PEM water electrolysis (Masa & Schuhmann, 2019). This remains a barrier to commercial hydrogen production using water electrolysis (Yu *et al*., 2018). This implies that electrocatalysts have to be designed to address these challenges.

Both OER and HER require large overpotentials to overcome the kinetic barriers as a result of high activation energies needed for reaction intermediates formation on the electrode surface, as well as to drive the reaction at a specific current density, mostly a geometric current density of 10 mA cm^{-2} is used as a benchmark. Electrocatalysts are used to lower the overpotential or activation energy of an electrochemical reaction (Seitz et al., 2016).

Considerable research efforts have been made recently in developing cheap and earth abundant electrocatalysts having high catalytic activity and good durability with some approaching commercial criteria.

Some recent research and development efforts have aimed at synthetic procedures and strategies for enhancing the performance of HER electrocatalysts like transition- metal phosphides, phosphosulfide and layered transition-metal dichalcogenides (WS_2 and MoS_2) (Yu *et al*., 2018). This implies that stable and robust HER electrocatalysts are currently being developed.

Bifunctional electrocatalysts are less likely to achieve HER and OER with low cost, sufficient efficiency and good stability. Most HER electrocatalysts can be active in acidic electrolytes, while the majority of OER electrocatalysts are only stable in basic electrolytes. The mismatch due to wide pH range needs to be addressed to design novel bifunctional electrocatalysts for water electrolysis (Fabbri et al., 2014b).

2.7. Electrodeposition of metallic and metal oxide films.

Electrodeposition of metals and metal oxides has been practiced since the 19^{th} century. In terms of controlling the thickness, structure and morphology of oxide electrodes, electrodeposition provides unique flexibility (Andricacos et al., 1989; Pompei et al., 2009). Electrodeposition of nickel and cobalt oxide onto graphite electrodes is important for alkaline water electrolysis.(X. Li et al., 2016; Wang et al., 2016)

Electrodeposition is currently applied in environmentally friendly low-cost solar cells production, solid oxide fuel cells, supercapacitors and recycling of metals (Arunachalam & Al Mayouf, 2018; Walter et al., 2010). Voltammetry, involving the application of a constant current (galvanostatic), constant potential (potentiostatic), or variable current – potential (potential versus current curves, or vice versa) is commonly used in electrodeposition. In electrodeposition, charge efficiency is a very important aspect used to determine the efficiency and amount of deposited material. (Fajardo *et al*., 2016). This means that the quality of the deposited film depends on the deposition parameters used.

In metal oxide electrodeposition, metal dissolution (an electrochemical step) and a chemical process due to precipitation of hydroxide on the substrate surface are involved. During metal or metal oxide electrodeposition, a fixed current or potential is imposed resulting in the formation of metal or metal oxide layers whose thickness and properties can be varied by the duration of the electrodeposition, concentration of the ions in the source electrolyte and the applied deposition parameters. Electrodeposition of a platinum group metal on a cheaper support enhances their electrocatalytic properties through electronic catalyst-support interactions and reduces the amounts of platinum group metal required. (X. Li *et al*., 2016). This implies that electrodeposition provides an option of reducing the cost of producing an otherwise expensive electrocatalyst by depositing it on cheaper substrates. For technology development, electrodeposition is still a paramount topic. Metallic or metal oxide films with different characteristics are obtained through adjusting operating parameters like electrodeposition cycles, electrodeposition time and concentration of the electrodeposition bath. In solar cells, both p-type and n-type are cheaply and flexibly produced using electrodeposition. Electrodeposition is also deployed in the recycling of spent batteries thus rendering it important for environmental conservation. NiO_x electrodeposited from nickel (II) amine complexes resulted in very stable uniform films during long-term catalytic cycling (Singh *et al*., 2013). This implies that the use of electrodeposition is an important technique in electrocatalysis.

2.8. Nickel metalloid alloys as electrocatalysts in water splitting

Nickle-metalloid (B, Si, P, As, Te, In and Ga) alloys are a highly promising emergent class of electrocatalysts for OER that can be synthesized from earth abundant and affordable resources. They thus provide an opportunity for transition from rare and expensive electrocatalysts like platinum and noble metal oxides like RuO_2 and IrO_2 (Masa *et al*., 2019). This implies that research

on optimization and understanding the performance of nickel-metalloid alloys is of topical importance (Seitz et al., 2016). Understanding the chemistries of these electrocatalysts that bestow upon them their interesting electrocatalytic properties is an important quest in current research in order to optimize their performance and ultimately foster mass hydrogen production (Andricacos et al., 1989; Fu et al., 2009).

2.9. Relationship between current and potential.

In order to determine the oxygen evolution reaction activity of the nickel metalloid alloy electrocatalyst films, the relationship between current and potential was utilized. The relationship between the current density (j) and the reaction overpotential (η) of an electrochemical reaction is described by the Butler-Volmer relationship according to equation (8),and the Tafel equation (10). The Butler-Volmer equation describes how the electrical current through an electrode (GC) depends on the voltage difference between the electrode and the bulk electrolyte (1 M NaOH) for a simple, unimolecular redox reaction, considering that both a cathodic and an anodic reaction occur on the same electrode.

$$j = j_0 \left\{ exp\left[\frac{\alpha_a z F \eta}{RT}\right] - exp\left[\frac{-\alpha_c z F \eta}{RT}\right] \right\} \ldots \ldots\ldots \textbf{\textit{Equation (8)}}$$

Where;

- j: electrode current density, $mA\ cm^{-2}$ (defined as

  $$j = \frac{current\ (I)}{electrode\ area\ (s)})$$

- j_o: exchange current density, $mA\ cm^{-2}$
- E electrode potential, V

- E_{eq}: equilibrium potential, V
- T absolute temperature, K
- z : number of electrons involved in the electrode reaction
- F: Faraday constant
- R: universal gas constant
- $\propto_c$: cathodic charge transfer coefficient, dimensionless
- $\propto_a$: anodic charge transfer coefficient, dimensionless
- η :activation overpotential (defined as $E - E_{eq}$).

At low overpotential region when $E \approx E_{eq}$, the Butler-Volmer equation (8) simplifies to

$$j = j_0 \frac{zF}{RT} \left(E - E_{eq}\right) \ldots\ldots\ldots\ldots\ldots\ldots\ldots\ldots \textbf{\textit{Equation (9)}}$$

At high overpotential region for an anodic reaction when $E \gg E_{eq}$ the Butler-Volmer equation (8) simplifies to the Tafel equation (10).

$$\eta = a + b_a log j \ldots\ldots\ldots\ldots\ldots\ldots\ldots\ldots\ldots\ldots \textbf{\textit{Equation (10)}}$$

Where a and b are Tafel equation constants for a given reaction at a specific temperature (25˚C in this study). The experimental set up is as shown in Figure 12 in the Appendix.

CHAPTER THREE

MATERIALS AND METHODS

3.1. Chemicals and reagents

Pre-synthesized nickel boride powder (NiB), nickel phosphide powder (NiP) and nickel telluride powder (NiTe) used as reference materials were received in a ready to use form from Ruhr University, Germany. Chemical reagents of analytical grade were received from commercial suppliers and were used without further modifications and treatments. These included: nickel (II) nitrate, gallium (II) nitrate and indium (II) nitrate used for co-electrodeposition. Nickel chloride, potassium hexacyanoferrate (II), potassium hexacyanoferrate (III), potassium chloride, 95% ethanol and sodium hydroxide for making the electrolyte. Micro polish alumina powder (0.05, 0.3 and 1.0 micron) used on the polishing cloth for polishing the glassy carbon electrode was from CHI instruments, USA. Distilled water was used as a solvent for all the experiments.

3.2. Equipment

All the electrochemical measurements were performed on a CHI 710E series electrochemical analyser. That is for electrochemical analysis as well as for preparation of nickel metalloid alloy electrocatalysts by electrodeposition method.

A standard three electrode one-compartment electrochemical cell with one platinum electrode as counter electrode (CE), a glassy carbon electrode with 4 mm diameter (electrode area 0.1256 cm^2) as working electrode (WE) and a silver-silver chloride (Ag/AgCl) electrode- as reference electrode (RE) against which all potentials in this work are referenced. Glassy carbon electrode was used as a substrate for catalyst support because relative OER inactivity at moderate overpotentials. A

photograph of the main setup of the electrochemical equipment used in this work and lay out of the various components is shown in Figure 12 in Appendix.

3.3. Methods

3.3.1. Preparation of reference electrocatalytic films by the drop coating method

For the nickel-metalloid alloy powder catalysts used for reference, 5 mg each of nickel boride (NiB), nickel terullide (NiTe) and nickel phosphide (NiP) powders were weighed into a centrifugation tube into which 500 µl of 95 % ethanol and 500 µl of distilled water were added. The suspension was then vigorously shaken for three minutes. For each sample, 5 µl of the suspension was drop coated on a clean glassy carbon (GC) electrode surface and allowed to dry for 30 min in air. Three GC electrodes were prepared in the same way each for NiB, NiTe and NiP.

3.3.2. Preparation of $Ni(OH)_2$, and nickel-metalloid (Ni-Ga and Ni-In) alloy films by electrodeposition

Electrodeposition of pure In, Ni and Ga films was performed in each case in 50 ml aqueous solution of 0.05 M indium (II) nitrate, nickel (II) chloride and gallium (II) nitrate, respectively on glassy carbon electrodes. $Ni(OH)_2$ was used as a positive control. The electrodeposition was achieved by performing 3,5,7, and 8 continuous cyclic voltammetry (CV) cycles with the CHI 710E series electrochemical analyzer in the potential range from -0.2 to - 0.8 V and a scan rate of 0.1 V/s, at room temperature. This was followed by co-electrodeposition from a mixture of 50 ml of 0.05 M indium (II) nitrate and nickel (II) chloride for synthesis of Ni-In films, and from a mixture of gallium (II) nitrate and nickel (II) chloride for synthesis of Ni-Ga films. After the electrodeposition processes, the films were rinsed with distilled water and left to dry in air for at least 30 mins.

3.3.3. Electrocatalytic activity for the oxygen evolution reaction

The OER activity of reference electrocatalytic films of NiB, NiTe and NiP powders were prepared as described by a procedure in Masa *et al*., (2019) and investigated using linear sweep voltammetry (LSV). This was done using the CHI 710E series electrochemical analyser by scanning the potential from an initial value of 0 V to 0.7 V, at a scan rate of 0.01 V/s, in a 1 M NaOH electrolyte solution at room temperature. NaOH electrolyte was chosen because of its activity and availability. The measurements were performed in a one-compartment electrochemical cell as shown in Figure 2 with a platinum electrode counter electrode (CE), a glassy carbon electrode working electrode (WE) and a silver-silver chloride (Ag/AgCl) reference electrode.

The OER activity of the resulting reference electrocatalytic films for the various nickel metalloid alloys (NiTe, NiB and NiP) was recorded as current against potential plots. The current for the OER was normalized by dividing it with the geometric area of the working electrode (glassy carbon, area = 0.1256 cm^2) to obtain the current density.

CHAPTER FOUR

RESULTS AND DISSCUSSION

4.1. Oxygen evolution reaction activity of nickel telluride, nickel boride and nickel phosphide powder catalysts

4.1.1 Oxygen evolution reaction activity of nickel telluride powder catalyst

Typical results of the OER activity of a NiTe electrocatalytic film recorded using LSV are shown in Figure 4. The data shows that at potentials below 0.39 V, no Faradaic current was observed. The measured background current was due to charging of the electrochemical double layer. Within this region, there was insufficient activation energy to initiate splitting of the water molecules. As the potential was increased to 0.4 V, a Faradic current attributed to the oxidation of Ni manifested. Between potentials of 0.4 and 0.6 V, the current was almost constant due to oxidation of nickel from $Ni^{2+}(Ni(OH)_2)$ to $Ni^{3+}(NiOOH)$, according to equation (11).

$$Ni(OH)_2(aq) \rightarrow NiOOH(aq) + H^+(aq) + e^- \ \ldots\ldots\ldots\textbf{\textit{Equation (11)}}$$

The NiOOH (nickel oxyhydroxide) intermediate is the active state of the catalyst. At potentials above 0.61 V, the current drastically increased more-less exponentially with further increase of the electrode potential in accordance with the Butler-Volmer relationship (equation 9). This is because of the fact that the driving force, electrode potential, was high enough to effect the electrolysis of water leading to the release of oxygen, which can be ascribed to the terminal step in the mechanism of oxygen evolution from oxidized metal surfaces represented by equation (12).

$$NiOOH\ (aq) + \ 2\ OH^-(aq) \rightarrow Ni(s) + \ O_2(g) + \ 2\ H_2\ O(l) + 2\ e^- \ldots\ldots\ \textbf{\textit{Equation (12)}}$$

4.1.2 Oxygen evolution reaction activity of nickel boride powder catalyst

The OER activity of a NiB electrocatalytic film recorded using LSV is shown in Figure 4. The data shows that at potentials below 0.37 V, no Faradaic current was observed. On increasing the potential to 0.38 V, a Faradaic current due to oxidation of Ni was observed. Between potentials of 0.38 and 0.57 V, the current was almost constant. At potentials above 0.58 V, the current drastically increased more-less exponentially with further increase of the electrode potential.

The potential corresponding to a current density of 10 mA cm^{-2} which is required for a 10% efficient solar water splitting device in 1M NaOH is commonly used as a figure of merit for comparing the performance of catalysts for the OER (McCrory *et al*., 2013). For the NiB catalyst investigated in this study, the potential required to deliver a current density of 10 mA cm^{-2} was 0.63 V. Taking $E_{RHE} = E_{Ag/AgCl} + 1.033$ as the conversion from the Ag/AgCl reference electrode scale to the reversible hydrogen electrode (RHE) scale (Niu et al., 2020), this would correspond to a potential of 1.66 V. This result compares well to recent data of 1.58 V reported in the literature for the OER of nickel boride materials (Masa *et al*., 2019).

4.1.3 Oxygen evolution reaction activity of nickel phosphide powder catalyst

The OER activity of the NiP drop coated electrocatalytic film recorded using LSV in NaOH (1 M) is shown in Figure 4. At potentials below 0.37 V, no Faradaic current was observed. There was onset of an oxidation wave at about 0.38 V as the potential was increased to more anodic potentials. Between potentials of 0.40 and 0.57 V, the current was almost constant. At potentials above 0.58 V, the current drastically increased more-less exponentially with further increase of the electrode potential. Above this potential, the electrode potential is sufficient to effect the electrolysis of water and more oxygen was evolved.

In order to enable easy comparison of the electrocatalytic activity of NiB, NiTe, and NiP powder catalysts, the OER activity curves of the three catalysts were plotted on one graph as shown in Figure 4.

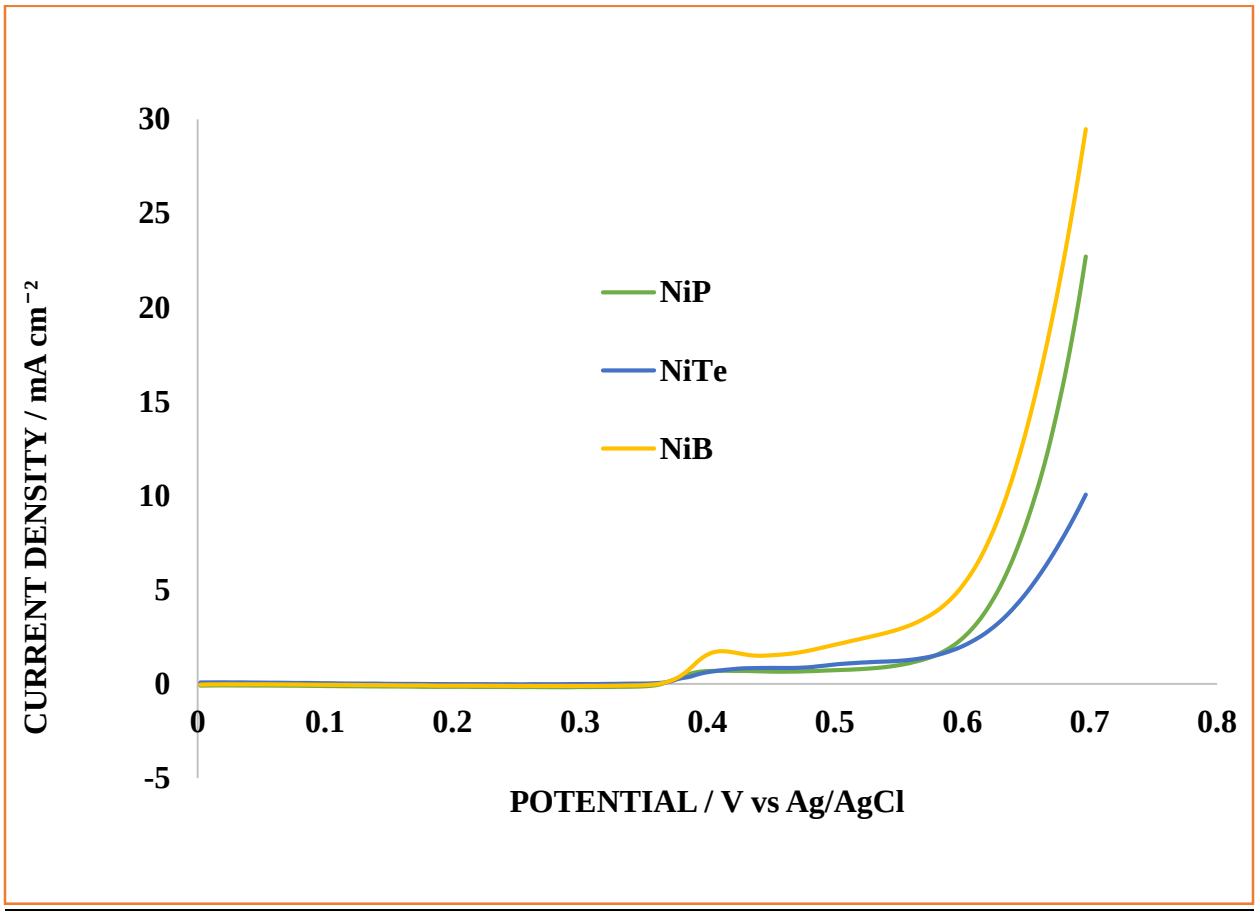

Figure 4 : *Comparison of the OER activity of NiB, NiTe and NiP electrocatalytic films.*

The data shows that at current density of 10 mA cm^{-2} NiB had the lowest potential of 0.627 V converted to reversible hydrogen electrode scale and therefore it was the best catalyst followed by NiP with 0.657 V and lastly NiTe with 0.697 V. From Figure 7, the $(Ni(OH)_2)$ film formed at 7 CV deposition cycles had a potential of 0.697 V corresponding to a current density of 10 mA cm^{-2}.

Taking $E_{RHE} = E_{Ag/AgCl} + 1.033$ as the conversion from the Ag/AgCl reference electrode scale to the reversible hydrogen electrode (RHE) scale (Niu et al., 2020) , this would correspond to the electrocatalytic activity in the order; $NiB\ (1.66\,V) > NiP\ (1.69\,V) > Ni \approx NiTe\ (1.73\,V)$ where a lower potential shows a higher catalytic activity.

A similar trend of observations of $NiB\ (1.58\,V) > NiP\ (1.59\,V) > Ni\ (1.62) > NiTe\ (1.63\,V)$ was reported by (Masa *et al*., 2019).

The results indicate that apart from NiTe which had the same activity as Ni, when Ni was modified with B or P this led to an overall increase in the OER electrocatalytic activity. NiB electrocatalyst exhibited the highest OER activity than NiP and NiTe because the reaction steps following hydroxylation reaction (equation 11) are considerably faster for NiB than for NiP and NiTe. This implies that the in-situ properties of the formed NiOOH OER active sites, is dependent on the type of metalloid under study. A notable influence of the metalloid element (B, P and Te) is alternation of the lattice structure of the host nickel metal as reported by (Masa *et al*., 2019).

Taking $Overpotential\ (\eta) = Potential\ vs\ RHE - 1.23$ as the expression for calculating the overpotential of an OER catalyst, it implies that the overpotentials of the catalysts at a current density of 10 mA cm^{-2} per geometric area in 1 M NaOH required for a 10 % efficient solar water- splitting device are in the order; $NiB\ (0.43\,V) > NiP\ (0.46\,V) > Ni \approx NiTe\ (0.5\,V)$. This compares well with the relevant figure of merit for benchmarking OER electrocatalysts at a current density of 10 mA cm^{-2} per geometric area in 1 M NaOH which was proposed by (McCrory *et al*., 2013) in which benchmark state -of - the art IrO_x catalyst and the promising earth abundant catalyst were reported to have overpotentials in the order $IrO_x\ (0.32 \pm 0.04\,V) > NiFeO_x\ (0.35 \pm 0.01\,V) > Ni\,O_x\ (\sim 0.36 - 0.43\,V) \geq NiCoO_x\ (0.38\,V) > NiCeO_x\ (0.43 \pm 0.03\,V)$.

The results obtained in this study further compares well with those reported by (McCrory *et al*., 2015) for Ru benchmark catalyst and other Pt- free OER electrocatalysts at a current density of 10 mA cm^{-2} per geometric area in 1 M NaOH in which the overpotentials were in the order; $Ru\ (0.29\ \pm 0.03\ V\ ) > NiMoFe\ (0.34\ \pm 0.02\ V)\ \approx\ NiFe\ (0.34\ \pm 0.02\ V\ )\ >$ $NiCo\ (0.42\ \pm 0.02\ V\ ) > Ni\ (0.47\ \pm 0.04\ V\ )$.

In 1 M NaOH , most catalysts including those in this study roughly operate with equivalent OER activity, achieving 10 mA cm^{-2} current densities necessary for a 10 % efficient solar water splitting device at overpotentials of $\eta = \sim 0.35 - 0.50\ V$.

4.2 Oxygen evolution reaction activity of nickel-gallium and nickel-indium electrocatalytic films formed by electrodeposition

In this section, results of the OER activity of Ni-Ga and Ni-In electrocatalytic films formed by electrodeposition are presented and discussed, together with the results of $Ni(OH)_2$ and the respective pure gallium (Ga) and indium (In) films as control samples. The electrocatalytic properties of films formed by electrodeposition depend on the applied deposition parameters, including, the concentration of the ions in the deposition bath, the applied electrodeposition method, duration of the electrodeposition, and the number of electrodeposition cycles in the case of electrodeposition by cyclic voltammetry (CV) (Fajardo *et al*., 2016). Since the CV method was used for electrodeposition in the current work, the effect of the number of CV deposition cycles on the OER performance was first investigated. Figure 5 shows a representative graph of electrodeposition curves of $Ni(OH)_2$ at 3 CV deposition cycles. The electrodeposition reaction of nickel takes place as shown in equations (13) and (14).

$$Ni^{2+}(aq) + 2e^- \rightarrow Ni(s) \ldots\ldots\ldots\ldots\ldots \quad \textbf{\textit{Equation (13)}}$$

$$Ni(s) + 2OH^{-}(aq) \rightarrow Ni(OH)_2(aq) + 2e^{-} \ldots\ldots\ldots\ldots\ldots\ldots\textbf{\textit{Equation (14)}}$$

During the cathodic scan (negative wards) from -0.2 V to -0.8 V, the potential can be seen to increase pronouncedly at -0.5 V until the lower vertex potential of -0.8 V was reached. This increase in current is ascribed to the electrochemical reduction of Ni^{2+} to Ni^{0}(equation 13). The current remained negative (lower than the initial background current) during the backward scan from -0.8 V to about -0.55 V, indicating that the electrodeposition process continues to take place even during the backward scan although with evidently lower intensity due to the lower current.

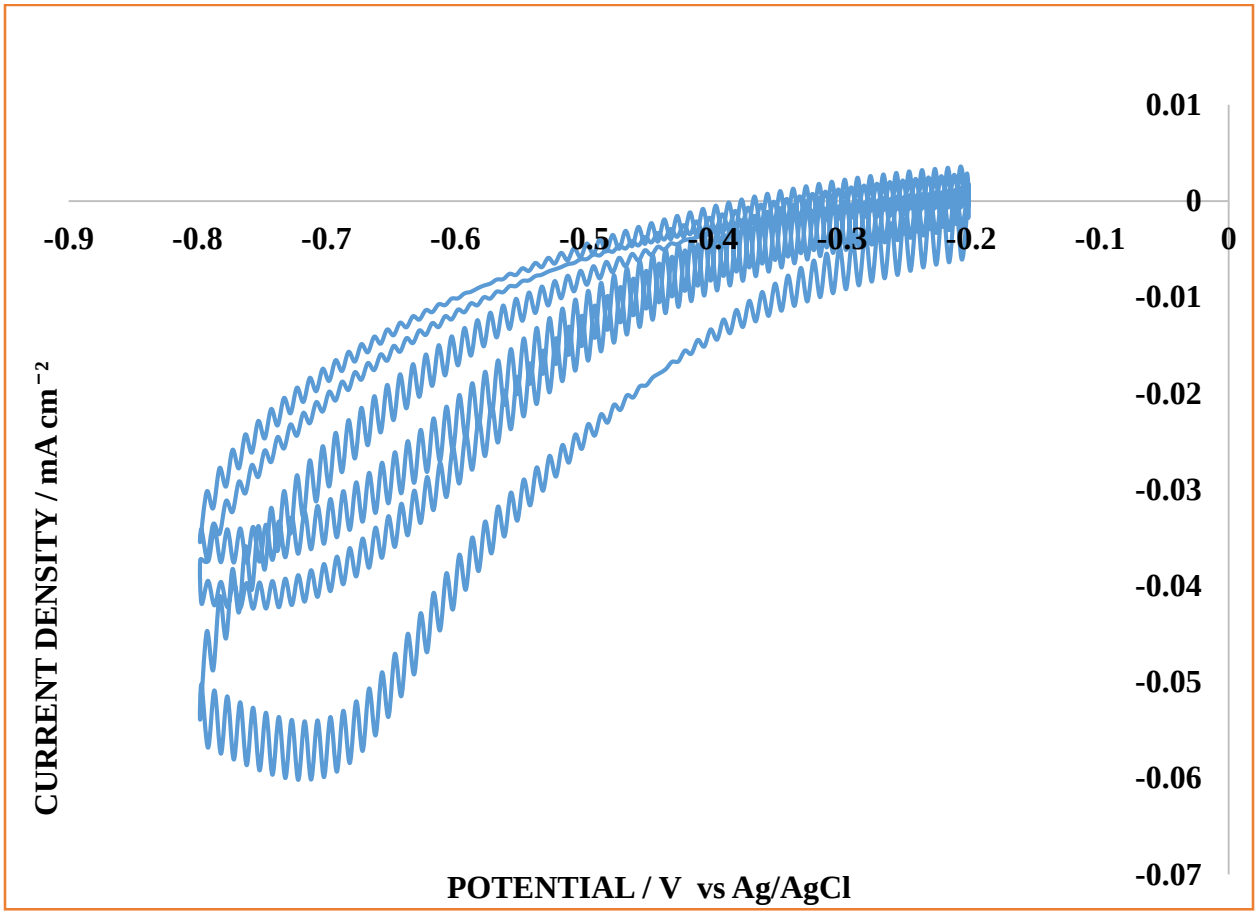

Figure 5: *Representative electrodeposition curves of $Ni(OH)_2$ electrocatalytic film (3 CV deposition cycles).*

4.2.1 Oxygen evolution reaction activity of nickel hydroxide electrocatalytic film formed by electrodeposition

The OER activity of electrocatalytic films of $Ni(OH)_2$ prepared as described in 3.3.2 was investigated using linear sweep voltammetry (LSV). The OER activity of the resulting $Ni(OH)_2$films was recorded as current against potential plots. The current for the OER was normalized with respect to the geometric area of the glassy carbon electrode (0.1256 cm^2) to obtain the current density.

Typical results of the OER activity of $Ni(OH)_2$ electrocatalytic film formed at 3 CV cycles recorded in NaOH (1 M) using LSV are shown in Figure 6a. The data shows that during the potential scan from 0 V to ≈ 0.37 V, no Faradaic current was observed below 0.38 V. The measured background current was due to charging currents in the electrochemical double layer. Below this potential, the electrode potential was insufficient to initiate splitting of the water molecules. As the potential was increased above 0.38 V, a Faradaic current due to oxidation of nickel was observed. Between potentials of 0.4 and 0.56 V, the current was almost constant due to oxidation of nickel from $Ni^{2+}(Ni(OH)_2)$ to $Ni^{3+}(NiOOH)$, according to equation (11). At potentials above 0.57 V, the current drastically increased more-less exponentially with further increase of the electrode potential in accordance with the Butler-Volmer relationship (equation 9). This is because of the fact that above this potential, the electrode is sufficiently active to effect the electrolysis of water and the rate of oxygen evolution increases with the applied electrode potential. Under these conditions, the evolution of oxygen is expected to be governed by equation (12), the terminal step in the mechanism of electrocatalytic oxygen evolution from metal oxide surfaces.

Since the number of deposition cycles influences the properties and activity of electrocatalytic films formed by electrodeposition, similar OER activity measurements were repeated for $Ni(OH)_2$ films formed by 5,7 and 8 electrodeposition cycles to determine the optimal number of deposition cycles with the highest OER activity. To enable easy comparison of the electrocatalytic activity of $Ni(OH)_2$ films for the different CV deposition cycles (3, 5, 7 and 8), the OER activities of the respective cycles were plotted on one Figure. The individual OER activity curves for 5, 7 and 8 deposition cycles can be found as Figure 13a, 13b and 13c respectively in the Appendix. Results of an overlay plot that was used to compare the effect of the number of CV deposition cycles on the OER activity of $Ni(OH)_2$ films are shown in Figure 6b.

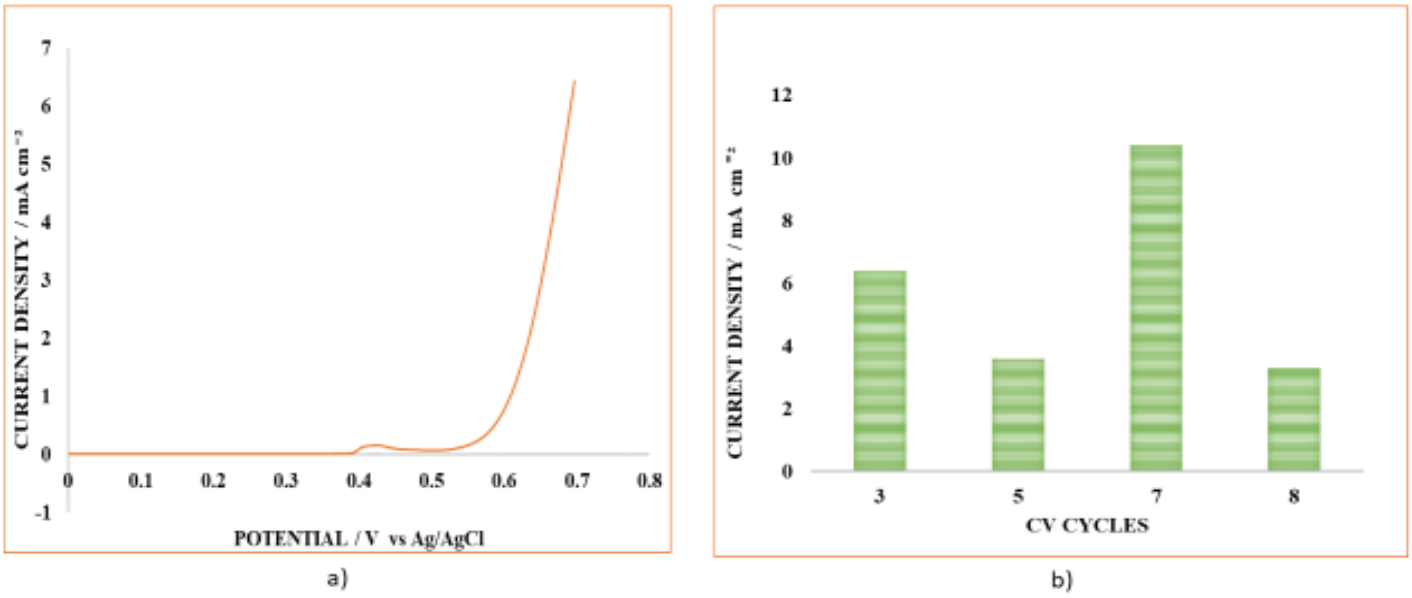

Figure 6: *a) The OER activity of $Ni(OH)_2$ electrodeposited electrocatalytic film formed at 3 CV cycles. b) A bar graph for comparison of the OER activity of $Ni(OH)_2$ films at 0.7 V for 3,5,7 and 8 CV electrodeposition cycles.*

The data in Table 2 shows that at 0.7 V, the $Ni(OH)_2$ electrocatalytic film formed at 7 CV deposition cycles had the highest OER activity affording a current density of 10.4 mA cm^{-2} followed by the $Ni(OH)_2$ electrocatalytic film formed at 3 CV deposition cycles with 6.4 mA cm^{-2}, then 5 CV deposition cycles with 3.6 mA cm^{-2} and lastly the $Ni(OH)_2$ electrocatalytic film formed at 8 CV deposition cycles with 3.3 mA cm^{-2} had the lowest performance. Subsequently, for comparison of the performance of $Ni(OH)_2$ with other catalysts, the OER activity curve and performance of the film formed by 7 deposition cycles was used. Further analysis of the data shows that $Ni(OH)_2$ electrocatalytic film at a current density of 10 mA cm^{-2} had a potential of 0.697 V. A conversion of this potential to the RHE scale gave a potential of 1.73 V (Niu et al., 2020).

Table 2 : *OER activity of $Ni(OH)_2$, $In(OH)_2$, and $Ga(OH)_2$ films formed at 3,5,7 and 8 CV electrodeposition cycles.*

NUMBER OF CV DEPOSITION CYCLES AT 0.7V	**CURRENT DENSITY OF ELECTROCATALYTIC FILM (mA cm^{-2})**		
	$Ni(OH)_2$	$In(OH)_2$	$Ga(OH)_2$
3	6.4	0.15	0.09
5	3.6	0.12	0.08
7	10.4	0.08	0.1
8	3.3	0.06	0.07

4.2.2 Oxygen evolution reaction activity of gallium hydroxide electrocatalytic films formed by electrodeposition

The OER activity of electrocatalytic films of $Ga(OH)_2$ prepared as described in 3.3.2 was investigated using linear sweep voltammetry (LSV) in NaOH (1 M). The OER activity of the resulting electrocatalytic films for each of the $Ga(OH)_2$ was recorded. The electrodeposition reaction of gallium takes place as shown in equations (15) and (16).

$$Ga^{2+}(aq) + 2e^{-} \rightarrow Ga(s) \ldots\ldots\ldots\ldots\ldots\ldots \textbf{\textit{Equation (15)}}$$

$$Ga(s) + 2OH^{-}(aq) \rightarrow Ga(OH)_2(aq) + 2e^{-} \ldots\ldots \textbf{\textit{Equation (16)}}$$

Typical results of the OER activity of $Ga(\mathrm{OH})_2$ electrocatalytic film formed at 3 CV deposition cycles using LSV are shown in Figure 7a. The data shows that at potentials below 0.39 V, no Faradaic current was observed. As the potential was increased to 0.4 V, a Faradaic current ascribed to oxidation of gallium was observed. Between potentials of 0.5 and 0.58 V, the current was almost constant due to oxidation of gallium from Ga^{2+} ($Ga(OH)_2$) to Ga^{3+} ($GaOOH$), according to equation (17).

$$Ga(OH)_2(aq) \rightarrow GaOOH(aq) + H^{+}(aq) + e^{-} \ldots\ldots\ldots \textbf{\textit{Equation (17)}}$$

At potentials above 0.58 V, the current drastically increased more-less exponentially with further increase of the electrode potential. Above this potential, the electrode potential was sufficiently high to effect the electrolysis of water evolving oxygen according to equation (18).

$$GaOOH(aq) + OH^{-}(aq) \rightarrow Ga(s) + O_2(g) + H_2O(l) + e^{-} \ldots. \textbf{\textit{Equation (18)}}$$

Similar OER activity measurements were repeated for $Ga(OH)_2$ films formed by 5,7 and 8 electrodeposition cycles to determine the optimal number of deposition cycles with the highest OER activity. To enable easy comparison of the electrocatalytic activity of $Ga(OH)_2$films for the different CV deposition cycles (3, 5, 7 and 8), the OER activity curves of the respective cycles were plotted on one graph. The individual OER activity curves for 5, 7 and 8 deposition cycles can be found as Figure 14a, 14b and 14c respectively in the Appendix. Results of an overlay plot

of the current density against potential that was used to compare the OER activity of the films formed by different number of CV deposition cycles are shown in Figure 7b.

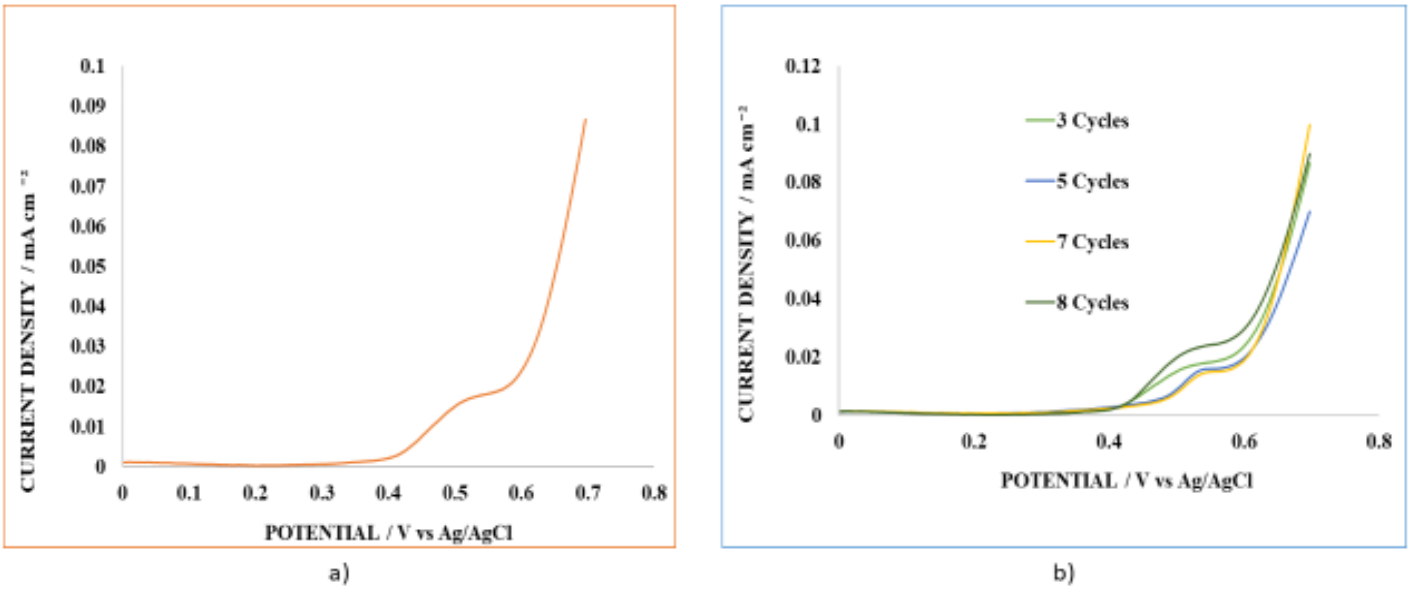

Figure 7: *a) The OER activity of* $Ga(OH)_2$ *electrodeposited electrocatalytic film formed at 3 CV cycles. b) Comparison of the OER activity of* $Ga(OH)_2$ *film electrodeposited on glassy carbon electrode by 3,5,7 and 8 CV electrodeposition cycles.*

The data in Table 2 shows that at 0.7 V, the $Ga(OH)_2$ electrocatalytic film formed at 7 CV deposition cycles had the highest activity with a current density of 0.1 mA cm^{-2} and therefore exhibited the highest performance followed by the $Ga(OH)_2$ electrocatalytic film formed at 3 CV deposition cycles with 0.09 mA cm^{-2}, then 5 CV deposition cycles with 0.08 mA cm^{-2} and lastly $Ga(OH)_2$ electrocatalytic film formed at 8 CV deposition cycles with 0.07 mA cm^{-2} had the lowest performance. Subsequently, for comparison of the performance of Ga with other

catalysts, the OER activity curve and performance of the film formed by 7 deposition cycles was used. The results show that the OER activity of the best Ga film at 7 deposition cycles did not reach the benchmarking current density of 10 mA cm^{-2}. Hence the need for alloy formation with Ni to form Ni-Ga which was expected to have an enhanced OER activity than that of Ni or Ga alone.

4.2.3. Oxygen evolution reaction activity of indium hydroxide electrocatalytic films formed by electrodeposition

The OER activity of the resulting electrocatalytic films for different CV deposition cycles was recorded. The electrodeposition reaction of indium takes place as shown in equations (19) and (20).

$$In^{2+}(aq) + 2e^{-} \rightarrow In(s) \quad \text{.....} \textbf{\textit{Equation (19)}}$$

$$In(s) + 2OH^{-}(aq) \rightarrow In(OH)_2(aq) + 2e^{-} \quad \text{.....} \textbf{\textit{Equation (20)}}$$

Typical results of the OER activity of $In(OH)_2$ electrocatalytic film formed at 3 CV deposition cycles are shown in Figure 8a. The data shows that at potentials below 0.38 V no Faradaic current was observed. As the potential was increased to 0.39 V, a Faradaic current ascribed to oxidation of indium was observed. At potentials above 0.39 V, the current drastically increased. Between potentials of 0.52 and 0.58 V, the current was almost constant due to oxidation of indium from In^{2+} ($In(OH)_2$) to In^{3+} (InOOH), according to equation (21).

$$In(OH)_2(aq) \rightarrow InOOH(aq) + H^{+}(aq) + e^{-} \quad \text{.....} \textbf{\textit{Equation (21)}}$$

At potentials above 0.58 V, the current drastically increased. Above this potential, the electrode potential was sufficiently high to effect the electrolysis of water evolving oxygen according to equation (22).

$InOOH(aq) + OH^{-}(aq) \rightarrow In(s) + O_2(g) + H_2O(l) + e^{-}$ …….**Equation (22)**

Similar OER activity measurements were repeated for $In(OH)_2$ films formed by 5,7 and 8 electrodeposition cycles to determine the optimal number of deposition cycles with the highest OER activity. For easy comparison of the electrocatalytic activity of $In(OH)_2$films for the different CV deposition cycles (3, 5, 7 and 8), the OER activity curves of the respective cycles were plotted on one graph. The individual OER activity curves for 5, 7 and 8 deposition cycles can be found as Figure 15a, 15b and 15c respectively in the Appendix. Results of an overlay plot that was used to compare the CV deposition cycles are shown in Figure 8b.

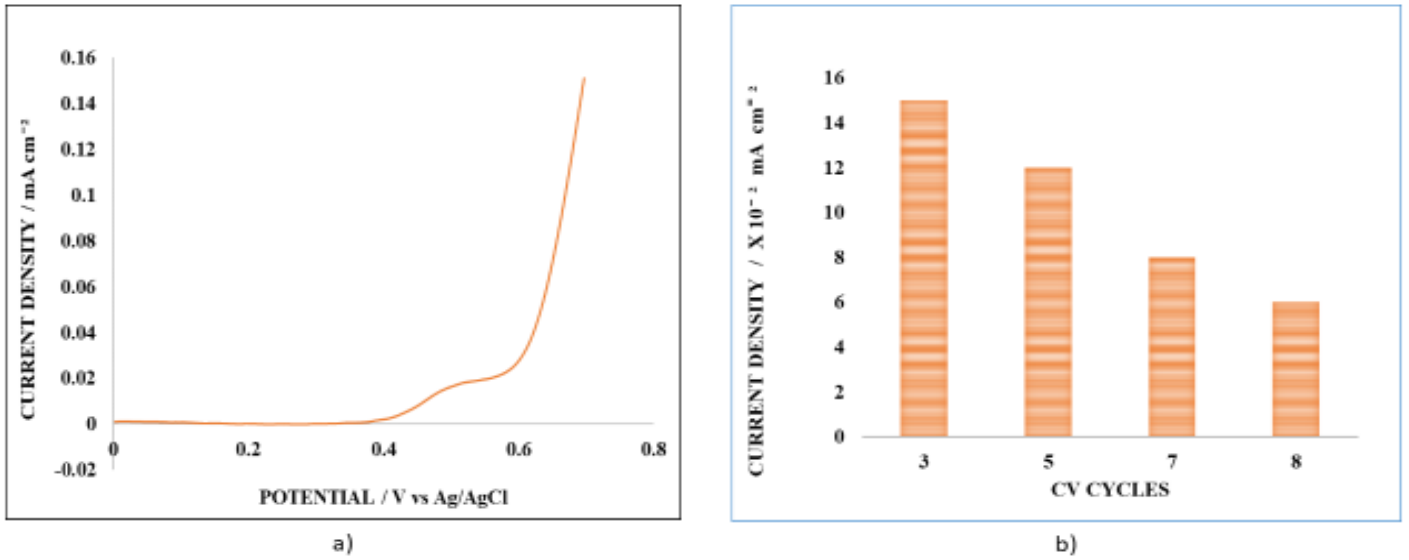

Figure 8: *a) The OER activity of $In(OH)_2$ electrodeposited electrocatalytic film formed at 3 CV cycles. b) Comparison of the OER activity of $In(OH)_2$ electrodeposited electrocatalytic films formed at 3,5,7 and 8 CV cycles respectively.*

The data in Table 2 shows that at $In(OH)_2$ electrocatalytic film formed at 3 CV deposition cycles had the highest activity and therefore it had the highest performance at 0.15 mA cm^{-2} followed by

$In(OH)_2$ electrocatalytic film formed at 5 CV deposition cycles with 0.12 mA cm^{-2}, this was followed by $In(OH)_2$ electrocatalytic film formed at 7 CV deposition cycles with 0.08 mA cm^{-2} and lastly $In(OH)_2$ electrocatalytic film formed at 8 CV deposition cycles with 0.06 mA cm^{-2} had the lowest performance. Subsequently, for comparison of the performance of pure $In(OH)_2$ with other catalysts, the OER activity curve and performance of the film formed by 3 deposition cycles was used. The results show that the OER activity of the best In film at 3 deposition cycles did not reach the benchmarking current density of 10 mA cm^{-2}. Hence the need for alloy formation with Ni to form Ni-In which was expected to have an enhanced OER activity than that of Ni or In alone.

4.2.4. Oxygen evolution reaction activity of nickel-indium composite electrocatalytic film formed by electrodeposition

OER activity of the resulting electrocatalytic films for each of the Ni-In composite was recorded. Typical results of the OER activity of Ni-In composite electrocatalytic film formed at 3 CV deposition cycles are shown in Figure 9a. The data shows that at potentials below 0.39 V there was no Faradaic current observed. As the potential was increased to 0.4 V, a faradaic current was observed. This is possibly due to oxidation of the Ni-In composite film. At potentials above 0.56 V, the current drastically increased.

Similar OER activity measurements were repeated for Ni-In films formed by 5,7 and 8 electrodeposition cycles to determine the optimal number of deposition cycles with the highest OER activity. For easy comparison of the electrocatalytic activity of Ni-In films for the different CV deposition cycles (3, 5, 7 and 8), the OER activity curves of the respective cycles were plotted on one graph. The individual OER activity curves for 5, 7 and 8 deposition cycles can be found as

Figure 16a, 16b and 16c respectively in the Appendix. Results of an overlay plot used to compare the CV deposition cycles are shown in Figure 9b.

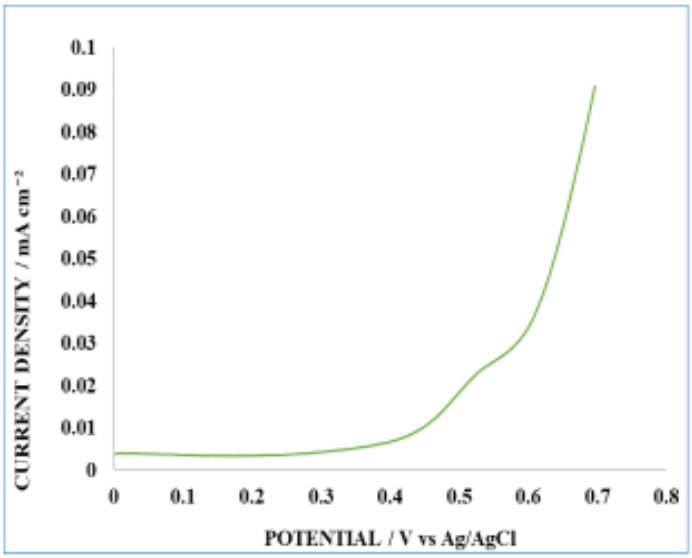

a)

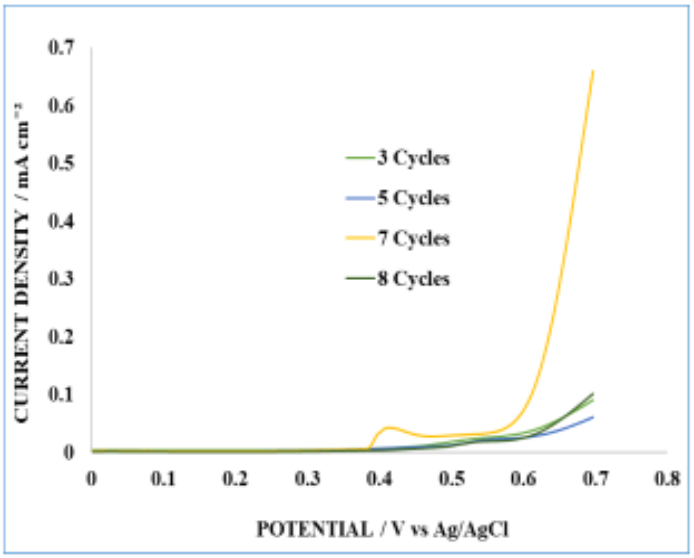

b)

Figure 9: *a) The OER activity of a Ni-In composite film electrodeposited by 3 CV cycles.*

b) Comparison of the OER activity of Ni- In composite films at 3,5,7 and 8 CV electrodeposition cycles respectively.

The data shows that at 0.7 V Ni-In electrocatalytic film formed at 7 CV deposition cycles had the highest activity with a current density of 0.66 mA cm^{-2} followed by Ni-In electrocatalytic film formed at 8 CV deposition cycles with 0.1 mA cm^{-2}, this was followed by Ni-In electrocatalytic film formed at 3 CV deposition cycles with 0.09 mA cm^{-2} and lastly Ni-In electrocatalytic film formed at 5 CV deposition cycles with 0.06 mA cm^{-2} had the lowest performance. Subsequently, for comparison of the performance of Ni-In with other catalysts, the OER activity curve and performance of the film formed by 7 deposition cycles was used. The results show that the OER

activity of the best Ni-In film at 7 deposition cycles did not reach the benchmarking current density of 10 mA cm^{-2}. This implies that there was no alloy formation between Ni and In which was expected to have an enhanced OER activity. This was probably due to the experimental conditions (room temperature) used in this study that did not favor alloy formation.

4.2.5. Oxygen evolution reaction activity of nickel-gallium composite electrocatalytic film formed by electrodeposition

OER activity of the resulting electrocatalytic films for each of the Ni-Ga composite was recorded. Typical results of the OER activity of Ni-Ga composite electrocatalytic film formed at 3 CV deposition cycles are shown in Figure 10a. The data shows that at potentials below 0.42 V there was no Faradaic current observed. As the potential was increased to 0.43 V, a Faradaic current ascribed to oxidation of Ni-Ga composite was observed. At potentials above 0.43 V, the current drastically increased more-less exponentially. Above this potential, the electrode potential was sufficiently high to effect the electrolysis of water evolving oxygen.

OER activity measurements were repeated for Ni-Ga films formed by 5,7 and 8 electrodeposition cycles. For comparison of the electrocatalytic activity of pure Ni-Ga films for the different CV deposition cycles (3, 5, 7 and 8), the OER activity curves of the respective cycles were plotted on one graph. The individual OER activity curves for 5, 7 and 8 deposition cycles can be found as Figure 17a,17b and 17c respectively in the Appendix. Results of an overlay plot used to compare

the effect of the different number of CV deposition cycles on the OER activity of the films are shown in Figure 10b.

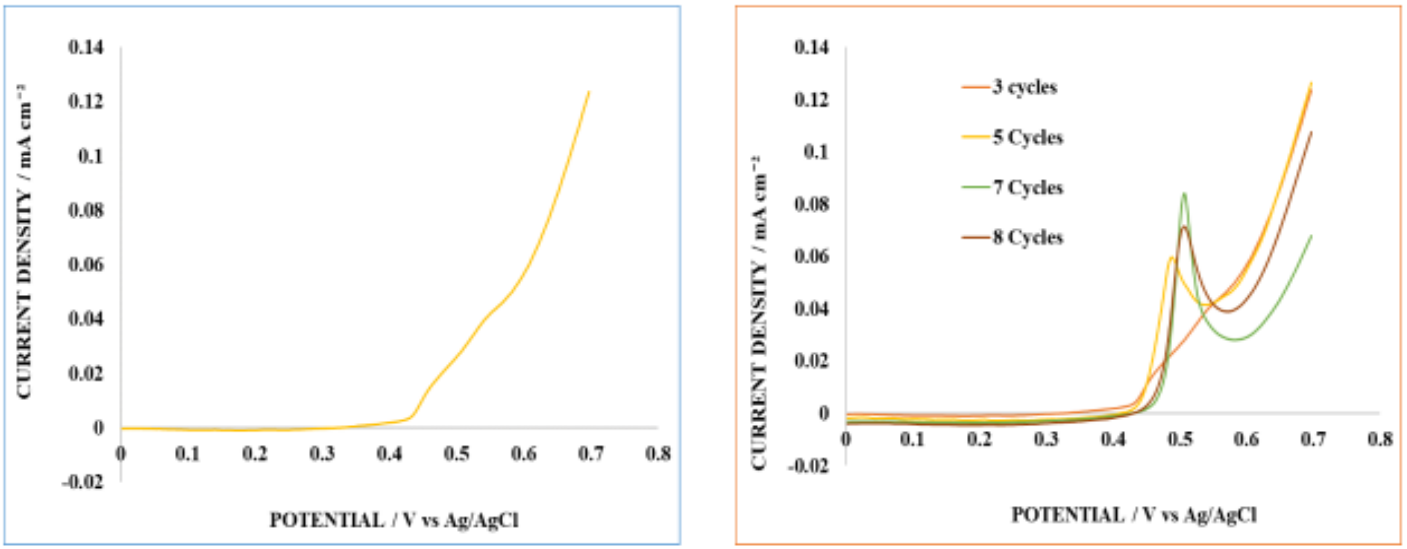

Figure 10 : *a) The OER activity of Ni-Ga composite electrodeposited electrocatalytic film formed at 3 CV cycles. b) Comparison of the OER activity of Ni-Ga composite films for 3,5,7 and 8 CV electrodeposition cycles.*

The data shows that at 0.7 V Ni-Ga electrocatalytic film formed at 5 CV deposition cycles had the highest activity at 0.13 mA cm^{-2} followed closely by Ni-Ga electrocatalytic film formed at 3 CV deposition cycles with 0.12 mA cm^{-2}, this was followed by Ni-Ga electrocatalytic film formed at 8 CV deposition cycles with 0.11 mA cm^{-2} and lastly Ni-Ga electrocatalytic film formed at 7 CV deposition cycles with 0.07 mA cm^{-2} had the lowest performance. Subsequently, for comparison of the performance of Ni-Ga with other catalysts, the OER activity curve and performance of the film formed by 5 deposition cycles was used. The results show that the OER

activity of the best Ni-Ga film at 5 deposition cycles did not reach the benchmarking current density of 10 mA cm^{-2}. This implies that there was no alloy formation between Ni and Ga which was expected to have an enhanced OER activity.

4.3. Comparison of the electrocatalytic activity of the nickel-indium and nickel – gallium composite electrocatalytic films

4.3.1. Comparison of the electrocatalytic activity of the nickel, gallium and nickel – gallium composite electrocatalytic films

For comparison of the electrocatalytic activity of the best Ni, Ga and Ni-Ga composite catalysts for CV deposition cycles that give the highest performance, the OER activity curves of the best respective cycles were plotted on one graph. Results of an overlay plot used to compare the best CV deposition cycles are shown in Figure 11b. The data shows that at 0.7 V Ni electrocatalytic film formed at 7 CV deposition cycles had the highest activity at 10.4 mA cm^{-2} followed by Ni-Ga composite electrocatalytic film formed at 5 CV deposition cycles with 0.13 mA cm^{-2}, this was lastly followed very closely by Ga electrocatalytic film formed at 7 CV deposition cycles with almost the same activity of 0.13 mA cm^{-2} and thus the lowest performance. It was expected from the hypothesis that the Ni-Ga films would perform better than Ni alone ($Ni(OH)_2$, however this was not the case. This indicates that at the conditions of the synthesis that were applied, it's most likely that there was no alloy formation of Ni-Ga. The low activity of Ni-Ga is possibly due to

the poor conductivity of Ga phase in the film since Ga is a semi-conductor. Alloy formation is expected to be achieved by annealing the films at high temperature ($\geq 500\ ℃$).

4.3.2 Comparison of the electrocatalytic activity of the nickel, indium and nickel – indium composite electrocatalytic films

Results of an overlay plot that was used to compare the best CV deposition cycles are shown in Figure 11a. The data shows that at 0.7 V Ni electrocatalytic film formed at 7 CV deposition cycles had the highest activity at 10.4 mA cm^{-2} followed by Ni-In composite electrocatalytic film formed at 7 CV deposition cycles with 0.66 mA cm^{-2}, this was lastly followed by In electrocatalytic film formed at 3 CV deposition cycles with activity of 0.15 mA cm^{-2} and thus the lowest performance. It was expected from the hypothesis that the Ni-In films would perform better than Ni alone, however this was a null hypothesis. This indicates that at the conditions of the synthesis that were applied, it is most likely that there was no alloy formation of Ni-In. The low activity of Ni-In is possibly due to the poor conductivity of the In phase or domains in the film since In is a semi-conductor.

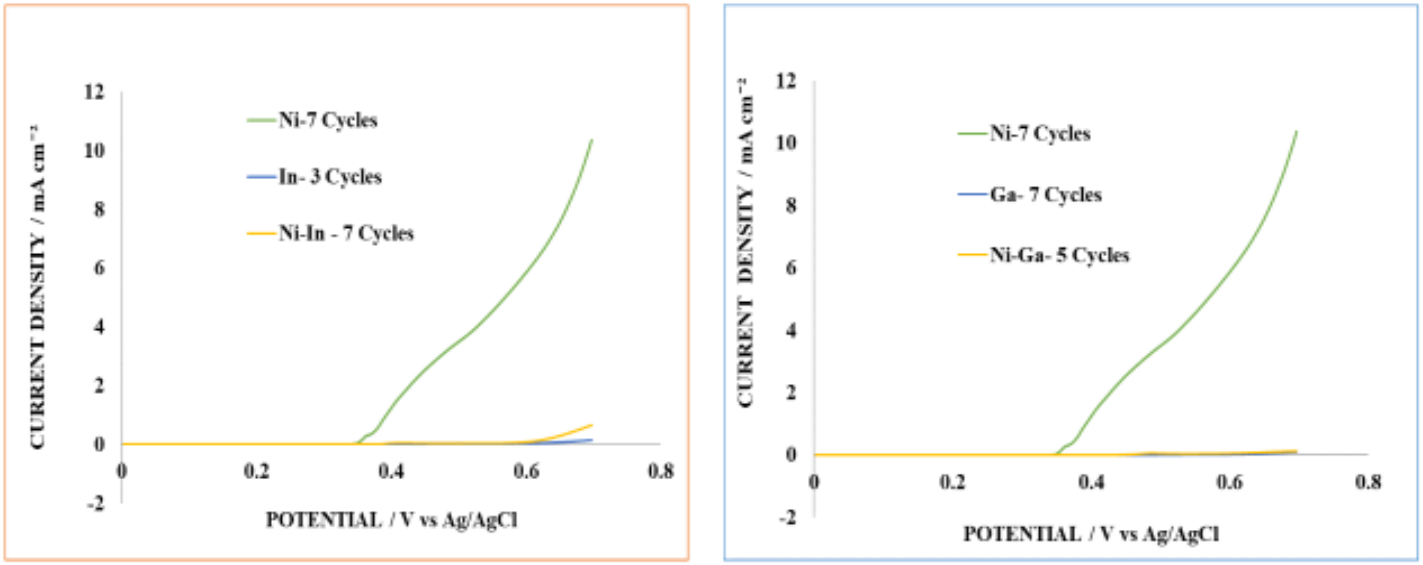

Figure 11 : *a) Comparison of the OER activity of electrodeposited films of Ni, In and Ni- In composite. b) Comparison of the OER activity of* $Ni(OH)_2$ *, Ga and Ni-Ga composite electrocatalytic films.*

CHAPTER FIVE

CONCLUSIONS AND RECOMMENDATIONS

5.1. Conclusions

In and Ni-Ga metalloid alloy films were prepared by electrochemical deposition. Investigation of the effect of the number of CV deposition cycles on the OER performance revealed that CV deposition cycles that had the highest activity and therefore the highest performance were; 7 for Ni, 7 for Ga ,3 for In ,7 for Ni-In and 5 for Ni-Ga composite electrocatalytic films respectively.

OER activity of electrodeposited Ni-In and Ni-Ga films in electrocatalytic water splitting was determined. The OER activity of $Ni(OH)_2$ films formed was several folds higher than that of the Ga and In films, as well as that of the composite Ni-Ga and Ni-In films. Ga and In species exist as discrete domains rather than alloys in the Ni-Ga and Ni-In composite films. The attempted method for synthesis of Ni-Ga and Ni-In alloy films by electrodeposition most likely led to the formation of Ni-Ga and Ni-In composite films with discrete domains of oxides of their respective elements but not alloys.

5.2. Recommendations

The following recommendations are made from this study;

1. Electrodeposition of electrocatalytic films should be done using the following CV deposition cycles that had the highest OER activity and therefore the highest performance; 7 for Ni, 7 for Ga ,3 for In ,7 for Ni-In and 5 for Ni-Ga electrocatalytic films respectively.

2. Future follow-up work should include a thermal treatment step of the films after electrochemical deposition.

REFERENCES

1. Andricacos, P. C., Arana, C., & Romankiw, L. T. (1989). *Electrodeposition of Nickel-Iron Alloys*. *136*(5), 1336–1340. Retrieved January 20, 2019
2. Armor, J. N. (2005). Catalysis and the hydrogen economy. In *Catalysis Letters*. Retrieved May 25, 2019, from https://doi.org/10.1007/s10562-005-4877-3
3. Arunachalam, P., & Al Mayouf, A. M. (2018). Photoelectrochemical Water Splitting. In *Noble Metal-Metal Oxide Hybrid Nanoparticles: Fundamentals and Applications*. Retrieved May 20, 2019, from https://doi.org/10.1016/B978-0-12-814134-2.00028-0
4. Bockris, J. O. M. (1972). A hydrogen economy. *Science*. Retrieved May 20, 2019 from https://doi.org/10.1126/science.176.4041.1323
5. Carmo, M., Fritz, D. L., Mergel, J., & Stolten, D. (2013). A comprehensive review on PEM water electrolysis. *International Journal of Hydrogen Energy*, *38*(12), 4901–4934.Retrieved May 20,2019 from https://doi.org/10.1016/j.ijhydene.2013.01.151
6. Crabtree, G. W., Dresselhaus, M. S., & Buchanan, M. V. (2004a). The hydrogen economy. In *Physics Today*. Retrieved February 19,2019 from https://doi.org/10.1063/1.1878333
7. Crabtree, G. W., Dresselhaus, M. S., & Buchanan, M. V. (2004b). The hydrogen economy. *Physics Today*, *57*(12), 39–44. Retrieved February 19,2019 from https://doi.org/10.1063/1.1878333
8. *Daily Metal Price: Ruthenium Price (USD / Kilogram) for the Last Day*. (n.d.). Retrieved January 31, 2021, from https://www.dailymetalprice.com/metalprices.php?c=ru&u=kg&d=1
9. Daly, B. P., & Barry, F. J. (2003). Electrochemical nickel-phosphorus alloy formation.

International Materials Reviews. Retrieved January 30,2020 from https://doi.org/10.1179/095066003225008482

10. de Vasconcelos, B. R., & Lavoie, J. M. (2019). Recent advances in power-to-X technology for the production of fuels and chemicals. *Frontiers in Chemistry*, *7*(JUN), 1–24. Retrieved May 25,2019 from https://doi.org/10.3389/fchem.2019.00392
11. Development, M. (2019). *Ministry of Energy and Mineral Development Draft National Energy Policy October 2019*. *October*. Retrieved January 25,2021
12. Fabbri, E., Habereder, A., Waltar, K., Kötz, R., & Schmidt, T. J. (2014a). Developments and perspectives of oxide-based catalysts for the oxygen evolution reaction. In *Catalysis Science and Technology*. Retrieved May 20,2019 from https://doi.org/10.1039/c4cy00669k
13. Fabbri, E., Habereder, A., Waltar, K., Kötz, R., & Schmidt, T. J. (2014b). Developments and perspectives of oxide-based catalysts for the oxygen evolution reaction. *Catalysis Science and Technology*, *4*(11), 3800–3821. Retrieved May 20,2019 from https://doi.org/10.1039/c4cy00669k
14. Fajardo, S., García-Galvan, R., F., Barranco, V., Galvan, J. C., & Batlle, S. F. (2016). We are IntechOpen , the world ’ s leading publisher of Open Access books Built by scientists , for scientists TOP 1 %. *Intech*, *i*(tourism), 13. Retrieved June 25,2019 from https://doi.org/http://dx.doi.org/10.5772/57353
15. Fu, G. R., Hu, Z. A., Xie, L. J., Jin, X. Q., Xie, Y. L., Wang, Y. X., Zhang, Z. Y., Yang, Y. Y., & Wu, H. Y. (2009). Electrodeposition of nickel hydroxide films on nickel foil and its electrochemical performances for supercapacitor. *International Journal of Electrochemical Science*, *4*(8), 1052–1062. Retrieved May 20,2019

16. Gangasingh, D., & Talbot, J. B. (1991). Anomalous Electrodeposition of Nickel-Iron. *Journal of The Electrochemical Society*, *138*(12), 3605–3611. Retrieved May 29,2020 from https://doi.org/10.1149/1.2085466

17. Guy, K. W. A. (2000). The hydrogen economy. *Process Safety and Environmental Protection*. Retrieved May 28, 2019 from https://doi.org/10.1205/095758200530709

18. Kuhl, K., Berkeley, L., & Cave, E. (2012). *Energy & New insights into the electrochemical reduction of carbon dioxide on metallic*. *May*. Retrieved June 25, 2019 from https://doi.org/10.1039/C2EE21234J

19. Li, J., Li, J., Zhou, X., Xia, Z., Gao, W., & Qu, Y. (2016). *Highly efficient and robust nickel phosphides as bifunctional electrocatalysts for overall water- splitting*. Retrieved June 26, 2019 from https://doi.org/10.1021/acsami.6b00731

20. Li, X., Hao, X., Abudula, A., & Guan, G. (2016). Nanostructured catalysts for electrochemical water splitting: Current state and prospects. *Journal of Materials Chemistry A*, *4*(31), 11973–12000. Retrieved May 03, 2019 from https://doi.org/10.1039/c6ta02334g

21. M., E., F.C., V., & Matencio, T. (2013). Metallic and Oxide Electrodeposition. *Modern Surface Engineering Treatments*. Retrieved May 2, 2019 from https://doi.org/10.5772/55684

22. Maeda, K., & Domen, K. (2010). Photocatalytic water splitting: Recent progress and future challenges. *Journal of Physical Chemistry Letters*. Retrieved May 20,2020 from https://doi.org/10.1021/jz1007966

23. Marbán, G., & Valdés-Solís, T. (2007). Towards the hydrogen economy? *International Journal of Hydrogen Energy*. Retrieved May 2,2019 from

https://doi.org/10.1016/j.ijhydene.2006.12.017

24. Masa, J., Piontek, S., Wilde, P., Antoni, H., Eckhard, T., Chen, Y., Muhler, M., Apfel, U., & Schuhmann, W. (2019). Ni-Metalloid (B, Si, P, As, and Te) Alloys as Water Oxidation Electrocatalysts. *Advanced Energy Materials*, *1900796*, 1900796. Retrieved June 25,2019 from https://doi.org/10.1002/aenm.201900796
25. Masa, J., & Schuhmann, W. (2019). The Role of Non-Metallic and Metalloid Elements on the Electrocatalytic Activity of Cobalt and Nickel Catalysts for the Oxygen Evolution Reaction. *ChemCatChem*, *11*(24), 5842–5854. Retrieved July 20,2020 from https://doi.org/10.1002/cctc.201901151
26. McCrory, C. C. L., Jung, S., Ferrer, I. M., Chatman, S. M., Peters, J. C., & Jaramillo, T. F. (2015). Benchmarking Hydrogen Evolving Reaction and Oxygen Evolving Reaction Electrocatalysts for Solar Water Splitting Devices. *Journal of the American Chemical Society*. Retrieved February 20,2019 from https://doi.org/10.1021/ja510442p
27. McCrory, C. C. L., Jung, S., Peters, J. C., & Jaramillo, T. F. (2013). Benchmarking heterogeneous electrocatalysts for the oxygen evolution reaction. *Journal of the American Chemical Society*. Retrieved May 29,2019 from https://doi.org/10.1021/ja407115p
28. Millet, P., Mbemba, N., Grigoriev, S. A., Fateev, V. N., Aukauloo, A., & Etiévant, C. (2011a). Electrochemical performances of PEM water electrolysis cells and perspectives. *International Journal of Hydrogen Energy*, *36*(6), 4134–4142. Retrieved July 10,2019 from https://doi.org/10.1016/j.ijhydene.2010.06.105
29. Millet, P., Mbemba, N., Grigoriev, S. A., Fateev, V. N., Aukauloo, A., & Etiévant, C. (2011b). Electrochemical performances of PEM water electrolysis cells and perspectives.

International Journal of Hydrogen Energy. Retrieved March 20,2019 from https://doi.org/10.1016/j.ijhydene.2010.06.105

30. Ngamlerdpokin, K., & Tantavichet, N. (2014). Electrodeposition of nickel-copper alloys to use as a cathode for hydrogen evolution in an alkaline media. *International Journal of Hydrogen Energy*. Retrieved June 28,2019 from https://doi.org/10.1016/j.ijhydene.2013.12.013
31. Ni, M., Leung, M. K. H., Leung, D. Y. C., & Sumathy, K. (2007). A review and recent developments in photocatalytic water-splitting using TiO2 for hydrogen production. In *Renewable and Sustainable Energy Reviews*. Retrieved July 2, 2019 from https://doi.org/10.1016/j.rser.2005.01.009
32. Niaz, S., Manzoor, T., & Pandith, A. H. (2015). Hydrogen storage: Materials, methods and perspectives. In *Renewable and Sustainable Energy Reviews*. Retrieved February 2, 2019 from https://doi.org/10.1016/j.rser.2015.05.011
33. Niu, S., Li, S., Du, Y., Han, X., & Xu, P. (2020). How to Reliably Report the Overpotential of an Electrocatalyst. *ACS Energy Letters*, *5*(4), 1083–1087. Retrieved May 25, 2019 from https://doi.org/10.1021/acsenergylett.0c00321
34. Oriňáková, R., Turoňová, A., Kladeková, D., Gálová, M., & Smith, R. M. (2006). Recent developments in the electrodeposition of nickel and some nickel-based alloys. *Journal of Applied Electrochemistry*, *36*(9), 957–972. Retrieved January 20,2019 from https://doi.org/10.1007/s10800-006-9162-7
35. Pompei, E., Magagnin, L., Lecis, N., & Cavallotti, P. L. (2009). Electrodeposition of nickel-BN composite coatings. *Electrochimica Acta*, *54*(9), 2571–2574. Retrieved March 20, 2019 from https://doi.org/10.1016/j.electacta.2008.06.034

36. Roger, I., Shipman, M. A., & Symes, M. D. (2017). Earth-abundant catalysts for electrochemical and photoelectrochemical water splitting. In *Nature Reviews Chemistry*. Retrieved February 25, 2019 from https://doi.org/10.1038/s41570-016-0003

37. Seitz, L. C., Dickens, C. F., Nishio, K., Hikita, Y., Montoya, J., Doyle, A., Kirk, C., Vojvodic, A., Hwang, H. Y., Norskov, J. K., & Jaramillo, T. F. (2016). A highly active and stable IrOx/SrIrO3catalyst for the Oxygen evolution reaction. *Science, 353*(6303), 1011–1014. Retrieved June 2, 2019 from https://doi.org/10.1126/science.aaf5050

38. Singh, A., Chang, S. L. Y., Hocking, R. K., Bach, U., & Spiccia, L. (2013). Highly active nickel oxide water oxidation catalysts deposited from molecular complexes. *Energy and Environmental Science, 6*(2), 579–586. Retrieved May 20,2020 from https://doi.org/10.1039/c2ee23862d

39. Suen, N. T., Hung, S. F., Quan, Q., Zhang, N., Xu, Y. J., & Chen, H. M. (2017). Electrocatalysis for the oxygen evolution reaction: Recent development and future perspectives. In *Chemical Society Reviews*. Retrieved November 20,2020 from https://doi.org/10.1039/c6cs00328a

40. Tahir, M., Pan, L., Idrees, F., Zhang, X., Wang, L., Zou, J. J., & Wang, Z. L. (2017). Electrocatalytic oxygen evolution reaction for energy conversion and storage: A comprehensive review. In *Nano Energy*. Retrieved December 20,2019 from https://doi.org/10.1016/j.nanoen.2017.05.022

41. Tee, S. Y., Win, K. Y., Teo, W. S., Koh, L. D., Liu, S., Teng, C. P., & Han, M. Y. (2017). Recent Progress in Energy-Driven Water Splitting. *Advanced Science, 4*(5). Retrieved July 12, 2019 from https://doi.org/10.1002/advs.201600337

42. Walter, M. G., Warren, E. L., McKone, J. R., Boettcher, S. W., Mi, Q., Santori, E. A., &

Lewis, N. S. (2010). Solar water splitting cells. *Chemical Reviews*, *110*(11), 6446–6473. Retrieved March 14, 2019 from https://doi.org/10.1021/cr1002326

43. Wang, J., Cui, W., Liu, Q., Xing, Z., Asiri, A. M., & Sun, X. (2016). Recent Progress in Cobalt-Based Heterogeneous Catalysts for Electrochemical Water Splitting. *Advanced Materials*, *28*(2), 215–230. Retrieved December 2, 2019 from https://doi.org/10.1002/adma.201502696
44. You, B., & Sun, Y. (2018). Innovative Strategies for Electrocatalytic Water Splitting [Research-article]. *Accounts of Chemical Research*, *51*(7), 1571–1580. Retrieved March 2, 2021 from https://doi.org/10.1021/acs.accounts.8b00002
45. Yu, F., Yu, L., Mishra, I. K., Yu, Y., Ren, Z. F., & Zhou, H. Q. (2018). Recent developments in earth-abundant and non-noble electrocatalysts for water electrolysis. *Materials Today Physics*, *7*, 121–138. Retrieved February 19,2020 from https://doi.org/10.1016/j.mtphys.2018.11.007
46. Zeng, K., & Zhang, D. (2010). Recent progress in alkaline water electrolysis for hydrogen production and applications. *Progress in Energy and Combustion Science*, *36*(3), 307–326. Retrieved August 20,2019 from https://doi.org/10.1016/j.pecs.2009.11.002

APPENDICES

The electrochemical experimental setup that was used in this study is as shown in Figure 12.

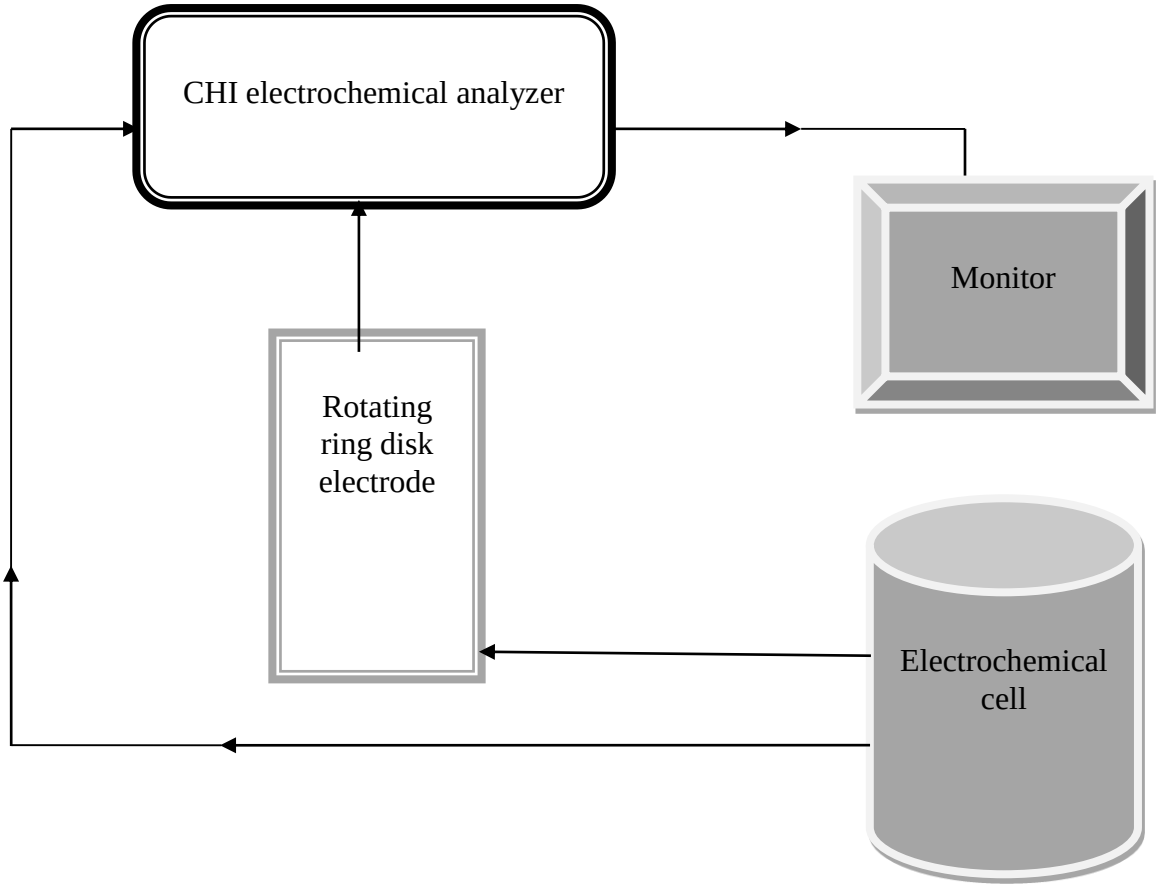

Figure 12: *A schematic diagrammatical representation of the electrochemical experimental setup used in this study.*

The OER activity curve of $Ni(OH)_2$ film formed at 5 CV, 7 CV and 8 CV deposition cycles was as shown in Figure 13a, 13b and 13c respectively.

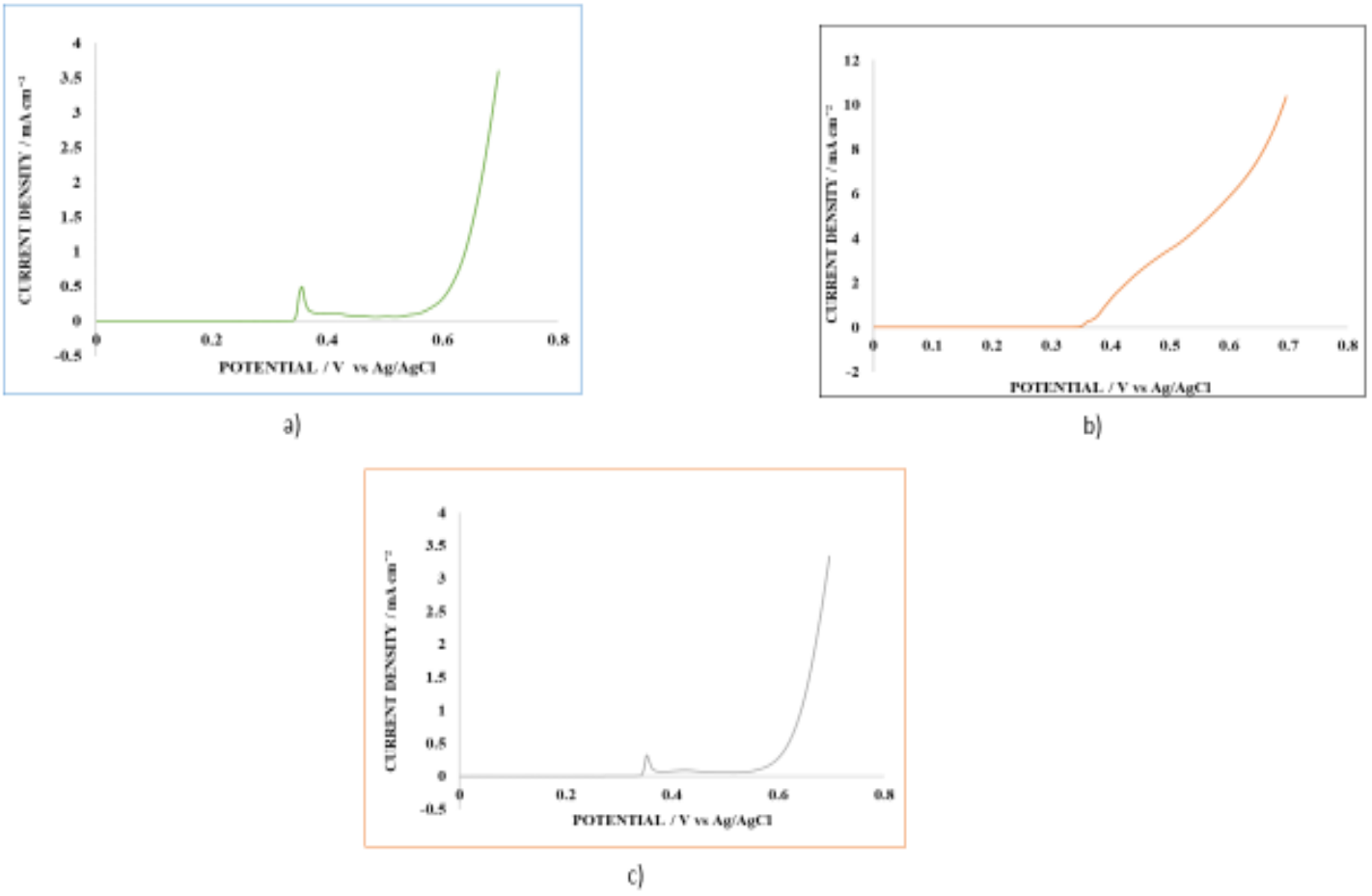

Figure 13: *The OER activity of $Ni(OH)_2$ electrodeposited electrocatalytic films; a) formed at 5 CV cycles, b) formed at 7 CV cycles and c) formed at 8 CV cycles .*

The OER activity curve of $Ga(OH)_2$ film formed at 5 CV, 7 CV and 8 CV deposition cycles was as shown in Figure 14a, 14b and 14c respectively.

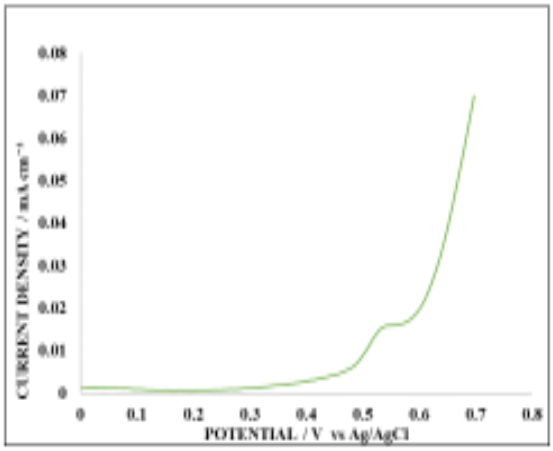

a)

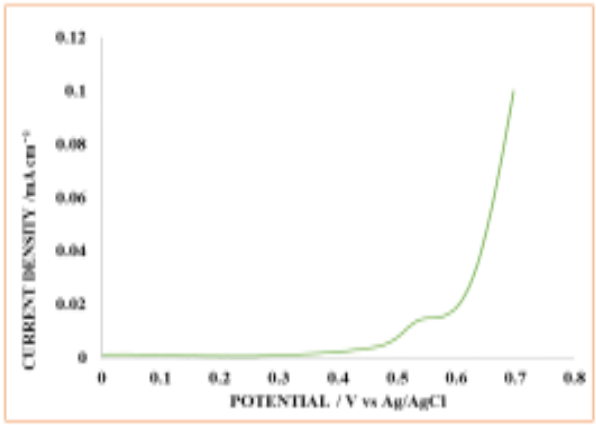

b)

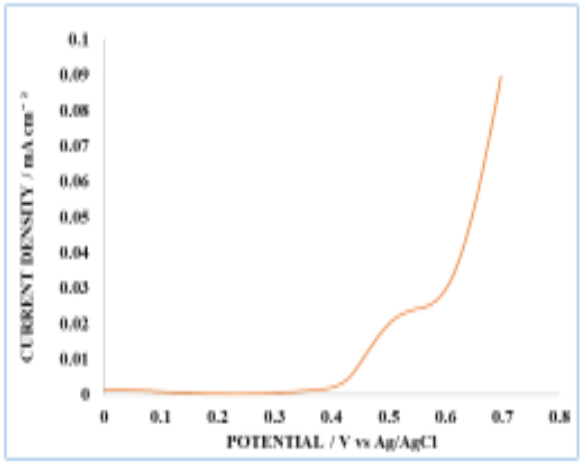

c)

Figure 14: *The OER activity of $Ga(OH)_2$ electrodeposited electrocatalytic films; a) formed at 5 CV cycles, b) formed at 7 CV cycles and c) formed at 8 CV cycles .*

The OER activity curve of $In(OH)_2$ film formed at 5 CV, 7 CV and 8 CV deposition cycles was as shown in Figure 15a, 15b and 15c respectively.

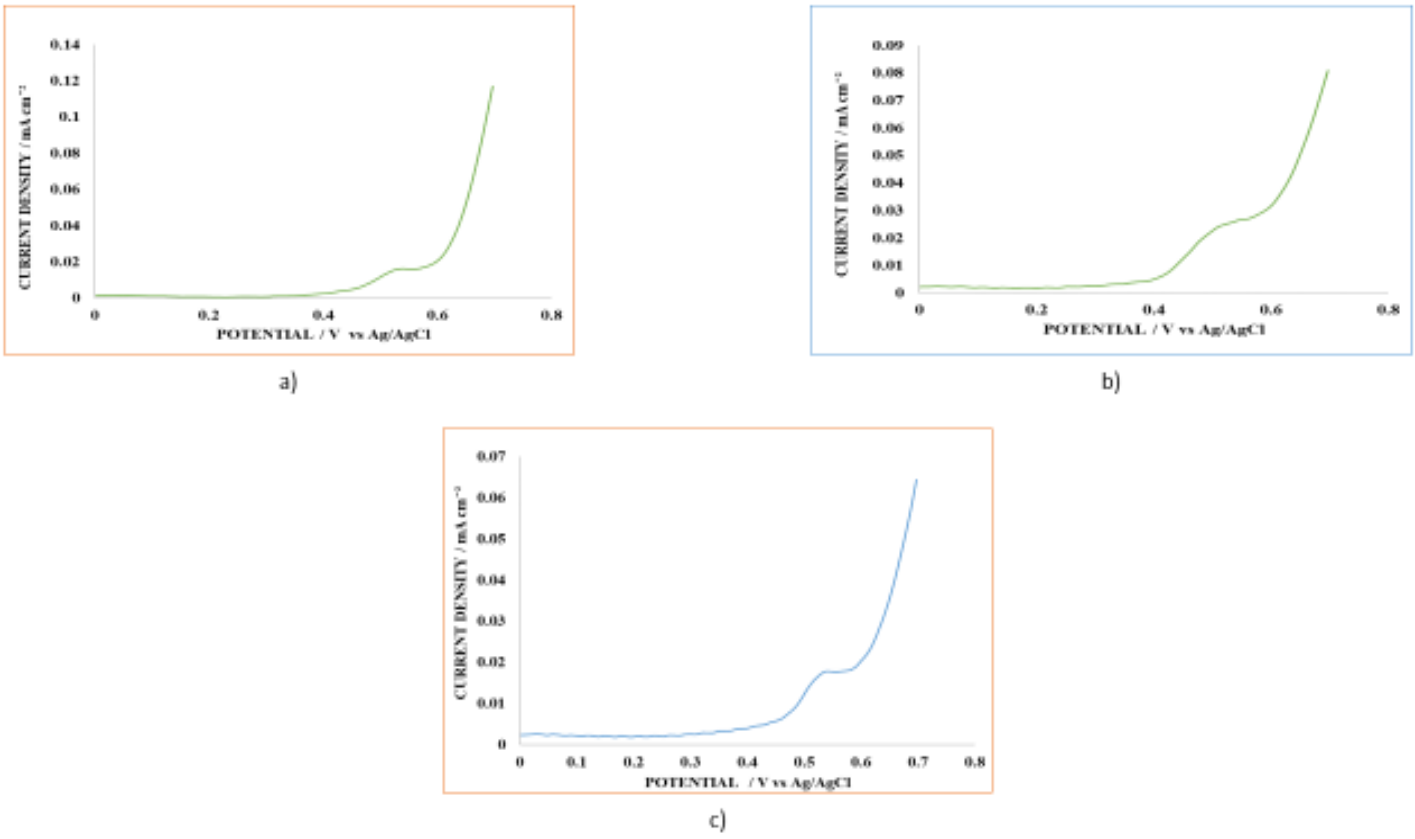

Figure 15: *The OER activity of $In(OH)_2$ electrodeposited electrocatalytic films; a) formed at 5 CV cycles , b) formed at 7 CV cycles and c) formed at 8 CV cycles.*

The OER activity curve of Ni- In composite film formed at 5 CV, 7 CV and 8 CV deposition cycles was as shown in Figure 16a, 16b and 16c respectively.

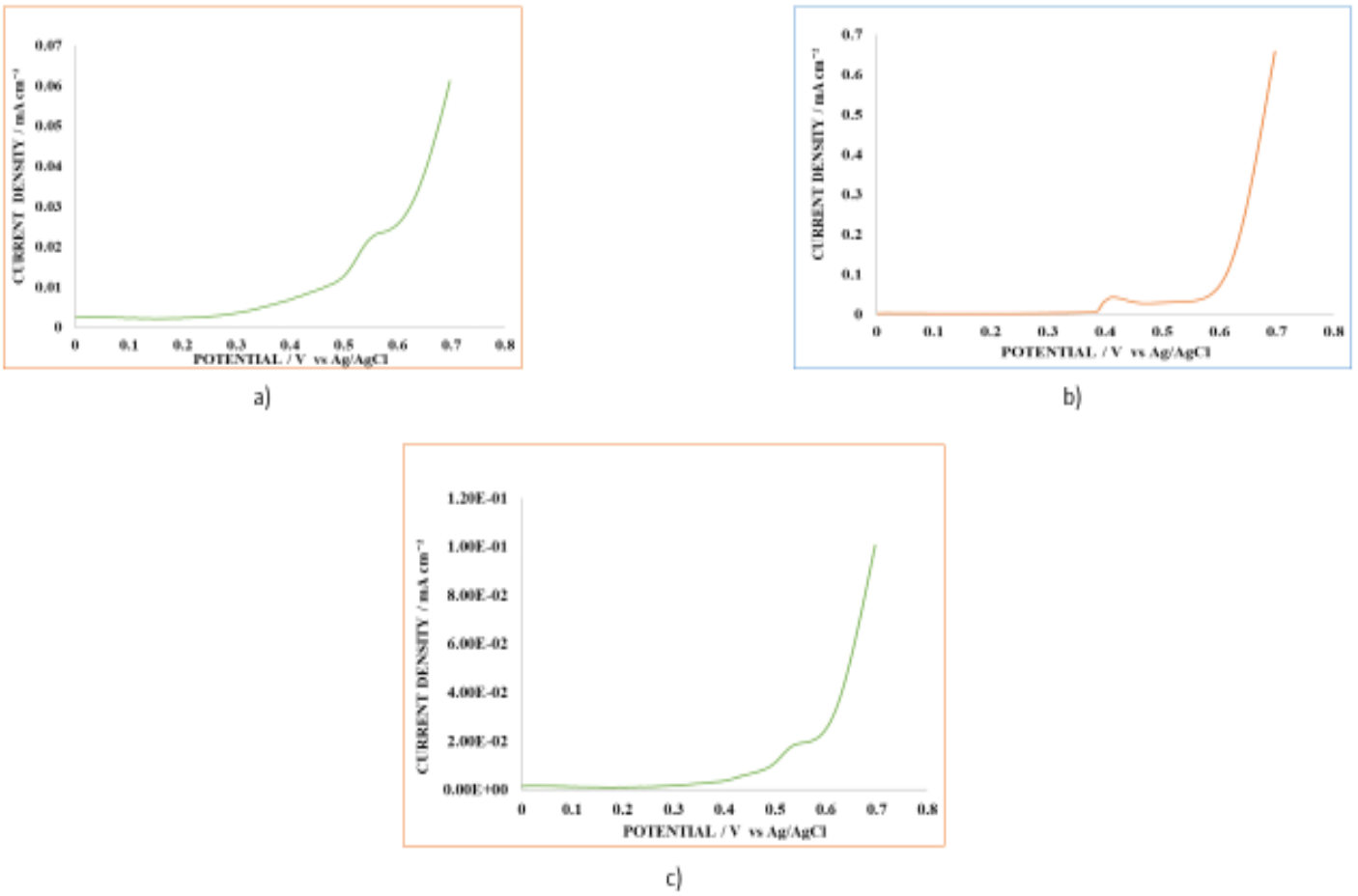

Figure 16: *The OER activity of Ni-In electrodeposited electrocatalytic film; a) formed at 5 CV cycles, b) formed at 7 CV cycles, and c) formed at 8 CV cycles .*

The OER activity curve of Ni- Ga composite film formed at 5 CV, 7 CV and 8 CV deposition cycles was as shown in Figure 17a, 17b and 17c respectively.

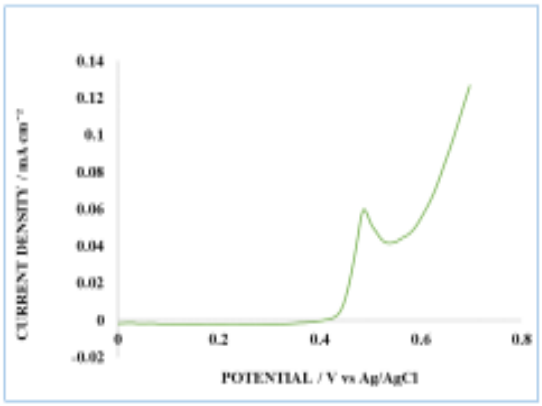

a)

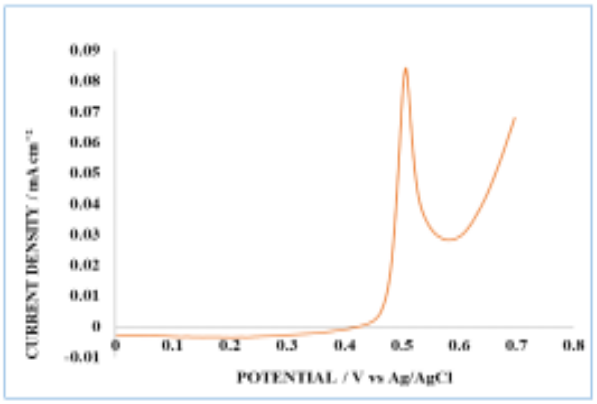

b)

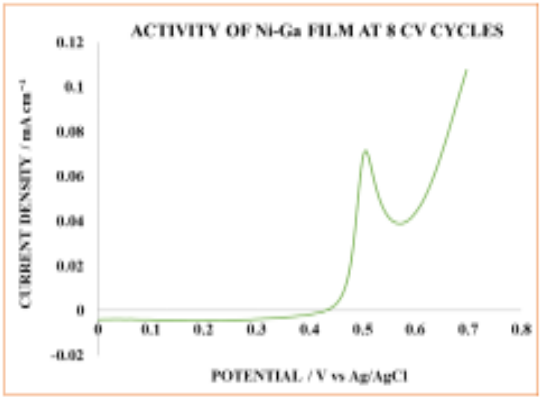

c)

Figure 17: *The OER activity of Ni-Ga electrodeposited electrocatalytic film; a) formed at 5 CV cycles b) formed at 7 CV cycles and c) formed at 8 CV cycles.*

Raw data.

The raw data obtained in this study is shown in tables 3-10.

Table 3: ***Oxygen evolution reaction activity of nickel boride using linear sweep voltammetry***

Potential/V	Current/A	Potential/V	Current/A	Potential/V	Current/A	Potential/V	Current/A
0.002	1.04E-07	0.177	1.90E-07	0.352	1.47E-07	0.527	-5.20E-06
0.007	8.48E-08	0.182	2.06E-07	0.357	1.01E-07	0.532	-5.37E-06
0.012	7.53E-08	0.187	2.18E-07	0.362	1.49E-08	0.537	-5.54E-06
0.017	7.22E-08	0.192	2.20E-07	0.367	-1.37E-07	0.542	-5.72E-06
0.022	6.44E-08	0.197	2.14E-07	0.372	-3.77E-07	0.547	-5.92E-06
0.027	6.59E-08	0.202	2.17E-07	0.377	-7.03E-07	0.552	-6.15E-06
0.032	6.67E-08	0.207	2.17E-07	0.382	-1.17E-06	0.557	-6.39E-06
0.037	7.06E-08	0.212	2.17E-07	0.387	-1.76E-06	0.562	-6.68E-06
0.042	6.59E-08	0.217	2.23E-07	0.392	-2.42E-06	0.567	-7.01E-06
0.047	7.06E-08	0.222	2.25E-07	0.397	-2.98E-06	0.572	-7.39E-06
0.052	7.06E-08	0.227	2.29E-07	0.402	-3.36E-06	0.577	-7.81E-06
0.057	7.38E-08	0.232	2.30E-07	0.407	-3.57E-06	0.582	-8.30E-06
0.062	8.01E-08	0.237	2.34E-07	0.412	-3.61E-06	0.587	-8.88E-06
0.067	7.85E-08	0.242	2.39E-07	0.417	-3.56E-06	0.592	-9.56E-06
0.072	8.63E-08	0.247	2.42E-07	0.422	-3.45E-06	0.597	-1.03E-05
0.077	9.10E-08	0.252	2.44E-07	0.427	-3.32E-06	0.602	-1.13E-05
0.082	9.65E-08	0.257	2.42E-07	0.432	-3.20E-06	0.607	-1.23E-05
0.087	1.04E-07	0.262	2.42E-07	0.437	-3.13E-06	0.612	-1.34E-05
0.092	1.12E-07	0.267	2.48E-07	0.442	-3.11E-06	0.617	-1.48E-05
0.097	1.16E-07	0.272	2.43E-07	0.447	-3.14E-06	0.622	-1.63E-05
0.102	1.23E-07	0.277	2.45E-07	0.452	-3.18E-06	0.627	-1.79E-05
0.107	1.26E-07	0.282	2.48E-07	0.457	-3.23E-06	0.632	-1.98E-05
0.112	1.36E-07	0.287	2.49E-07	0.462	-3.29E-06	0.637	-2.18E-05
0.117	1.37E-07	0.292	2.51E-07	0.467	-3.38E-06	0.642	-2.41E-05
0.122	1.48E-07	0.297	2.49E-07	0.472	-3.48E-06	0.647	-2.65E-05
0.127	1.48E-07	0.302	2.48E-07	0.477	-3.61E-06	0.652	-2.91E-05
0.132	1.60E-07	0.307	2.40E-07	0.482	-3.75E-06	0.657	-3.19E-05
0.137	1.60E-07	0.312	2.46E-07	0.487	-3.91E-06	0.662	-3.50E-05
0.142	1.65E-07	0.317	2.36E-07	0.492	-4.07E-06	0.667	-3.82E-05
0.147	1.66E-07	0.322	2.32E-07	0.497	-4.24E-06	0.672	-4.16E-05
0.152	1.73E-07	0.327	2.24E-07	0.502	-4.40E-06	0.677	-4.51E-05
0.157	1.85E-07	0.332	2.13E-07	0.507	-4.56E-06	0.682	-4.90E-05
0.162	1.89E-07	0.337	2.02E-07	0.512	-4.73E-06	0.687	-5.30E-05
0.167	1.95E-07	0.342	1.90E-07	0.517	-4.88E-06	0.692	-5.72E-05
0.172	1.86E-07	0.347	1.76E-07	0.522	-5.05E-06	0.697	-6.17E-05

Table 4: ***Oxygen evolution reaction activity of nickel phosphide using linear sweep voltammetry***

Potential/V	Current/A	Potential/V	Current/A	Potential/V	Current/A	Potential/V	Current/A
0.002	1.87E-07	0.182	3.24E-07	0.362	7.69E-08	0.542	-1.92E-06
0.007	1.81E-07	0.187	3.28E-07	0.367	-1.35E-07	0.547	-2.01E-06
0.012	1.72E-07	0.192	3.20E-07	0.372	-3.81E-07	0.552	-2.13E-06
0.017	1.67E-07	0.197	3.20E-07	0.377	-6.37E-07	0.557	-2.26E-06
0.022	1.66E-07	0.202	3.21E-07	0.382	-9.23E-07	0.562	-2.43E-06
0.027	1.69E-07	0.207	3.18E-07	0.387	-1.15E-06	0.567	-2.61E-06
0.032	1.73E-07	0.212	3.20E-07	0.392	-1.32E-06	0.572	-2.82E-06
0.037	1.73E-07	0.217	3.38E-07	0.397	-1.40E-06	0.577	-3.07E-06
0.042	1.76E-07	0.222	3.33E-07	0.402	-1.44E-06	0.582	-3.37E-06
0.047	1.77E-07	0.227	3.31E-07	0.407	-1.46E-06	0.587	-3.74E-06
0.052	1.79E-07	0.232	3.32E-07	0.412	-1.46E-06	0.592	-4.18E-06
0.057	1.82E-07	0.237	3.30E-07	0.417	-1.46E-06	0.597	-4.69E-06
0.062	1.85E-07	0.242	3.38E-07	0.422	-1.45E-06	0.602	-5.30E-06
0.067	1.93E-07	0.247	3.43E-07	0.427	-1.45E-06	0.607	-6.02E-06
0.072	1.97E-07	0.252	3.44E-07	0.432	-1.44E-06	0.612	-6.84E-06
0.077	1.97E-07	0.257	3.53E-07	0.437	-1.42E-06	0.617	-7.79E-06
0.082	2.03E-07	0.262	3.44E-07	0.442	-1.40E-06	0.622	-8.88E-06
0.087	2.14E-07	0.267	3.55E-07	0.447	-1.38E-06	0.627	-1.01E-05
0.092	2.16E-07	0.272	3.52E-07	0.452	-1.37E-06	0.632	-1.15E-05
0.097	2.26E-07	0.277	3.62E-07	0.457	-1.36E-06	0.637	-1.30E-05
0.102	2.36E-07	0.282	3.61E-07	0.462	-1.37E-06	0.642	-1.47E-05
0.107	2.41E-07	0.287	3.67E-07	0.467	-1.37E-06	0.647	-1.65E-05
0.112	2.48E-07	0.292	3.64E-07	0.472	-1.38E-06	0.652	-1.86E-05
0.117	2.54E-07	0.297	3.49E-07	0.477	-1.41E-06	0.657	-2.08E-05
0.122	2.57E-07	0.302	3.49E-07	0.482	-1.43E-06	0.662	-2.32E-05
0.127	2.61E-07	0.307	3.50E-07	0.487	-1.45E-06	0.667	-2.58E-05
0.132	2.72E-07	0.312	3.45E-07	0.492	-1.49E-06	0.672	-2.87E-05
0.137	2.75E-07	0.317	3.39E-07	0.497	-1.51E-06	0.677	-3.19E-05
0.142	2.76E-07	0.322	3.38E-07	0.502	-1.54E-06	0.682	-3.53E-05
0.147	2.86E-07	0.327	3.30E-07	0.507	-1.57E-06	0.687	-3.90E-05
0.152	2.84E-07	0.332	3.17E-07	0.512	-1.59E-06	0.692	-4.31E-05
0.157	2.89E-07	0.337	3.20E-07	0.517	-1.63E-06	0.697	-4.76E-05
0.162	2.97E-07	0.342	3.05E-07	0.522	-1.66E-06		
0.167	2.97E-07	0.347	2.87E-07	0.527	-1.71E-06		
0.172	3.11E-07	0.352	2.50E-07	0.532	-1.77E-06		
0.177	3.20E-07	0.357	1.86E-07	0.537	-1.83E-06		

Table 5: ***Oxygen evolution reaction activity of nickel telluride using linear sweep voltammetry***

Potential/V	Current/A	Potential/V	Current/A	Potential/V	Current/A	Potential/V	Current/A
0.002	-1.70E-07	0.187	1.10E-08	0.372	-3.30E-07	0.557	-2.65E-06
0.007	-1.74E-07	0.192	1.41E-08	0.377	-5.64E-07	0.562	-2.73E-06
0.012	-1.77E-07	0.197	1.33E-08	0.382	-6.94E-07	0.567	-2.84E-06
0.017	-1.83E-07	0.202	1.88E-08	0.387	-8.32E-07	0.572	-2.96E-06
0.022	-1.82E-07	0.207	1.73E-08	0.392	-1.06E-06	0.577	-3.10E-06
0.027	-1.74E-07	0.212	1.81E-08	0.397	-1.23E-06	0.582	-3.28E-06
0.032	-1.76E-07	0.217	2.04E-08	0.402	-1.35E-06	0.587	-3.49E-06
0.037	-1.74E-07	0.222	2.28E-08	0.407	-1.45E-06	0.592	-3.73E-06
0.042	-1.63E-07	0.227	2.20E-08	0.412	-1.54E-06	0.597	-4.00E-06
0.047	-1.58E-07	0.232	2.83E-08	0.417	-1.61E-06	0.602	-4.32E-06
0.052	-1.52E-07	0.237	3.14E-08	0.422	-1.68E-06	0.607	-4.68E-06
0.057	-1.44E-07	0.242	2.75E-08	0.427	-1.73E-06	0.612	-5.08E-06
0.062	-1.44E-07	0.247	3.14E-08	0.432	-1.75E-06	0.617	-5.53E-06
0.067	-1.37E-07	0.252	3.92E-08	0.437	-1.77E-06	0.622	-6.04E-06
0.072	-1.26E-07	0.257	3.45E-08	0.442	-1.78E-06	0.627	-6.61E-06
0.077	-1.15E-07	0.262	2.12E-08	0.447	-1.78E-06	0.632	-7.24E-06
0.082	-1.16E-07	0.267	2.28E-08	0.452	-1.79E-06	0.637	-7.94E-06
0.087	-1.15E-07	0.272	2.43E-08	0.457	-1.78E-06	0.642	-8.71E-06
0.092	-1.01E-07	0.277	2.28E-08	0.462	-1.78E-06	0.647	-9.53E-06
0.097	-8.87E-08	0.282	2.83E-08	0.467	-1.78E-06	0.652	-1.04E-05
0.102	-8.63E-08	0.287	2.04E-08	0.472	-1.80E-06	0.657	-1.14E-05
0.107	-7.85E-08	0.292	1.57E-08	0.477	-1.84E-06	0.662	-1.24E-05
0.112	-6.12E-08	0.297	1.02E-08	0.482	-1.89E-06	0.667	-1.35E-05
0.117	-5.34E-08	0.302	6.28E-09	0.487	-1.97E-06	0.672	-1.46E-05
0.122	-5.02E-08	0.307	5.49E-09	0.492	-2.04E-06	0.677	-1.58E-05
0.127	-4.55E-08	0.312	1.26E-08	0.497	-2.12E-06	0.682	-1.70E-05
0.132	-4.08E-08	0.317	-3.92E-09	0.502	-2.20E-06	0.687	-1.83E-05
0.137	-4.24E-08	0.322	-1.10E-08	0.507	-2.25E-06	0.692	-1.96E-05
0.142	-3.85E-08	0.327	-1.65E-08	0.512	-2.30E-06	0.697	-2.11E-05
0.147	-2.20E-08	0.332	-2.51E-08	0.517	-2.35E-06		
0.152	-1.57E-08	0.337	-3.85E-08	0.522	-2.39E-06		
0.157	-1.57E-08	0.342	-4.40E-08	0.527	-2.42E-06		
0.162	-6.28E-09	0.347	-4.40E-08	0.532	-2.46E-06		
0.167	-1.18E-08	0.352	-4.87E-08	0.537	-2.48E-06		
0.172	-6.28E-09	0.357	-7.61E-08	0.542	-2.51E-06		
0.177	-3.23E-13	0.362	-1.13E-07	0.547	-2.54E-06		
0.182	5.49E-09	0.367	-1.81E-07	0.552	-2.59E-06		

Table 6: ***Activity of pure nickel at 7 deposition cycles using linear sweep voltammetry***

Potential/V	Current/A	Potential/V	Current/A	Potential/V	Current/A	Potential/V	Current/A
0.002	-1.88E-08	0.187	-3.14E-09	0.372	-4.65E-05	0.557	-5.88E-04
0.007	-1.57E-08	0.192	2.35E-09	0.377	-5.97E-05	0.562	-6.03E-04
0.012	-2.43E-08	0.197	-3.23E-13	0.382	-7.87E-05	0.567	-6.19E-04
0.017	-3.45E-08	0.202	-1.88E-08	0.387	-1.02E-04	0.572	-6.36E-04
0.022	-5.49E-08	0.207	-4.63E-08	0.392	-1.23E-04	0.577	-6.52E-04
0.027	-5.97E-08	0.212	-6.28E-08	0.397	-1.42E-04	0.582	-6.69E-04
0.032	-6.99E-08	0.217	-8.16E-08	0.402	-1.63E-04	0.587	-6.86E-04
0.037	-5.89E-08	0.222	-9.73E-08	0.407	-1.82E-04	0.592	-7.03E-04
0.042	-3.85E-08	0.227	-1.07E-07	0.412	-1.99E-04	0.597	-7.21E-04
0.047	-1.88E-08	0.232	-1.02E-07	0.417	-2.15E-04	0.602	-7.38E-04
0.052	-1.88E-08	0.237	-9.26E-08	0.422	-2.31E-04	0.607	-7.56E-04
0.057	-2.98E-08	0.242	-8.40E-08	0.427	-2.47E-04	0.612	-7.75E-04
0.062	-3.85E-08	0.247	-8.24E-08	0.432	-2.63E-04	0.617	-7.94E-04
0.067	-5.89E-08	0.252	-8.87E-08	0.437	-2.79E-04	0.622	-8.14E-04
0.072	-6.44E-08	0.257	-1.25E-07	0.442	-2.94E-04	0.627	-8.35E-04
0.077	-5.73E-08	0.262	-1.63E-07	0.447	-3.08E-04	0.632	-8.56E-04
0.082	-3.61E-08	0.267	-1.97E-07	0.452	-3.22E-04	0.637	-8.80E-04
0.087	-6.28E-09	0.272	-2.17E-07	0.457	-3.35E-04	0.642	-9.04E-04
0.092	1.02E-08	0.277	-2.32E-07	0.462	-3.48E-04	0.647	-9.29E-04
0.097	9.42E-09	0.282	-2.57E-07	0.467	-3.61E-04	0.652	-9.56E-04
0.102	-3.14E-09	0.287	-2.77E-07	0.472	-3.73E-04	0.657	-9.85E-04
0.107	-2.67E-08	0.292	-2.94E-07	0.477	-3.85E-04	0.662	-1.02E-03
0.112	-2.98E-08	0.297	-3.12E-07	0.482	-3.97E-04	0.667	-1.05E-03
0.117	-3.45E-08	0.302	-3.29E-07	0.487	-4.08E-04	0.672	-1.08E-03
0.122	-3.45E-08	0.307	-3.44E-07	0.492	-4.19E-04	0.677	-1.12E-03
0.127	-2.12E-08	0.312	-3.63E-07	0.497	-4.30E-04	0.682	-1.16E-03
0.132	-1.57E-09	0.317	-3.91E-07	0.502	-4.41E-04	0.687	-1.20E-03
0.137	1.57E-08	0.322	-4.24E-07	0.507	-4.51E-04	0.692	-1.25E-03
0.142	2.04E-08	0.327	-4.74E-07	0.512	-4.62E-04	0.697	-1.30E-03
0.147	9.42E-09	0.332	-5.49E-07	0.517	-4.74E-04		
0.152	-3.92E-09	0.337	-6.66E-07	0.522	-4.86E-04		
0.157	-2.51E-08	0.342	-9.54E-07	0.527	-5.00E-04		
0.162	-3.38E-08	0.347	-2.08E-06	0.532	-5.14E-04		
0.167	-4.16E-08	0.352	-8.10E-06	0.537	-5.28E-04		
0.172	-4.08E-08	0.357	-1.97E-05	0.542	-5.42E-04		
0.177	-3.14E-08	0.362	-3.37E-05	0.547	-5.57E-04		
0.182	-1.18E-08	0.367	-3.89E-05	0.552	-5.72E-04		

Table 7: ***Activity of gallium at 7 deposition cycles using linear sweep voltammetry***

Potential/V	Current/A	Potential/V	Current/A	Potential/V	Current/A	Potential/V	Current/A
0.002	-1.41E-07	0.187	-6.91E-08	0.372	-2.14E-07	0.557	-1.86E-06
0.007	-1.50E-07	0.192	-6.75E-08	0.377	-2.28E-07	0.562	-1.87E-06
0.012	-1.52E-07	0.197	-6.67E-08	0.382	-2.36E-07	0.567	-1.88E-06
0.017	-1.54E-07	0.202	-6.36E-08	0.387	-2.57E-07	0.572	-1.90E-06
0.022	-1.55E-07	0.207	-6.28E-08	0.392	-2.68E-07	0.577	-1.93E-06
0.027	-1.49E-07	0.212	-6.91E-08	0.397	-2.75E-07	0.582	-1.99E-06
0.032	-1.53E-07	0.217	-6.36E-08	0.402	-2.79E-07	0.587	-2.06E-06
0.037	-1.55E-07	0.222	-5.97E-08	0.407	-2.91E-07	0.592	-2.15E-06
0.042	-1.56E-07	0.227	-6.28E-08	0.412	-3.03E-07	0.597	-2.26E-06
0.047	-1.51E-07	0.232	-6.36E-08	0.417	-3.23E-07	0.602	-2.41E-06
0.052	-1.51E-07	0.237	-6.51E-08	0.422	-3.44E-07	0.607	-2.58E-06
0.057	-1.44E-07	0.242	-6.59E-08	0.427	-3.56E-07	0.612	-2.81E-06
0.062	-1.45E-07	0.247	-6.28E-08	0.432	-3.73E-07	0.617	-3.06E-06
0.067	-1.43E-07	0.252	-5.97E-08	0.437	-3.84E-07	0.622	-3.35E-06
0.072	-1.41E-07	0.257	-5.97E-08	0.442	-4.08E-07	0.627	-3.68E-06
0.077	-1.32E-07	0.262	-6.44E-08	0.447	-4.24E-07	0.632	-4.06E-06
0.082	-1.26E-07	0.267	-7.77E-08	0.452	-4.51E-07	0.637	-4.47E-06
0.087	-1.26E-07	0.272	-8.55E-08	0.457	-4.73E-07	0.642	-4.95E-06
0.092	-1.26E-07	0.277	-8.48E-08	0.462	-4.96E-07	0.647	-5.48E-06
0.097	-1.15E-07	0.282	-8.87E-08	0.467	-5.20E-07	0.652	-6.05E-06
0.102	-1.16E-07	0.287	-9.42E-08	0.472	-5.66E-07	0.657	-6.64E-06
0.107	-1.19E-07	0.292	-9.34E-08	0.477	-6.02E-07	0.662	-7.27E-06
0.112	-1.14E-07	0.297	-9.89E-08	0.482	-6.61E-07	0.667	-7.95E-06
0.117	-1.04E-07	0.302	-1.01E-07	0.487	-7.23E-07	0.672	-8.66E-06
0.122	-9.73E-08	0.307	-1.13E-07	0.492	-7.96E-07	0.677	-9.37E-06
0.127	-9.03E-08	0.312	-1.13E-07	0.497	-8.86E-07	0.682	-1.01E-05
0.132	-8.48E-08	0.317	-1.15E-07	0.502	-9.90E-07	0.687	-1.09E-05
0.137	-8.48E-08	0.322	-1.23E-07	0.507	-1.11E-06	0.692	-1.17E-05
0.142	-8.08E-08	0.327	-1.28E-07	0.512	-1.24E-06	0.697	-1.25E-05
0.147	-7.85E-08	0.332	-1.39E-07	0.517	-1.38E-06		
0.152	-8.63E-08	0.337	-1.55E-07	0.522	-1.49E-06		
0.157	-8.16E-08	0.342	-1.67E-07	0.527	-1.60E-06		
0.162	-7.53E-08	0.347	-1.73E-07	0.532	-1.70E-06		
0.167	-7.53E-08	0.352	-1.81E-07	0.537	-1.77E-06		
0.172	-7.38E-08	0.357	-1.91E-07	0.542	-1.81E-06		
0.177	-6.75E-08	0.362	-1.95E-07	0.547	-1.84E-06		
0.182	-6.59E-08	0.367	-2.09E-07	0.552	-1.85E-06		

Table 8: ***Activity of indium at 3 deposition cycles using linear sweep voltammetry***

Potential/V	Current/A	Potential/V	Current/A	Potential/V	Current/A	Potential/V	Current/A
0.002	-1.07E-07	0.187	1.41E-08	0.372	-7.38E-08	0.557	-2.47E-06
0.007	-1.19E-07	0.192	9.42E-09	0.377	-9.34E-08	0.562	-2.52E-06
0.012	-1.26E-07	0.197	-3.14E-09	0.382	-1.28E-07	0.567	-2.58E-06
0.017	-1.29E-07	0.202	3.92E-09	0.387	-1.64E-07	0.572	-2.64E-06
0.022	-1.24E-07	0.207	7.85E-09	0.392	-1.88E-07	0.577	-2.72E-06
0.027	-1.18E-07	0.212	8.63E-09	0.397	-2.18E-07	0.582	-2.83E-06
0.032	-1.20E-07	0.217	1.65E-08	0.402	-2.45E-07	0.587	-2.95E-06
0.037	-1.11E-07	0.222	1.88E-08	0.407	-2.79E-07	0.592	-3.10E-06
0.042	-1.09E-07	0.227	2.90E-08	0.412	-3.27E-07	0.597	-3.29E-06
0.047	-1.04E-07	0.232	2.90E-08	0.417	-3.85E-07	0.602	-3.51E-06
0.052	-1.10E-07	0.237	2.43E-08	0.422	-4.53E-07	0.607	-3.79E-06
0.057	-1.06E-07	0.242	1.26E-08	0.427	-5.39E-07	0.612	-4.13E-06
0.062	-1.01E-07	0.247	1.02E-08	0.432	-6.19E-07	0.617	-4.51E-06
0.067	-9.89E-08	0.252	1.26E-08	0.437	-7.06E-07	0.622	-4.97E-06
0.072	-9.42E-08	0.257	1.26E-08	0.442	-7.97E-07	0.627	-5.50E-06
0.077	-8.63E-08	0.262	2.28E-08	0.447	-8.98E-07	0.632	-6.09E-06
0.082	-7.14E-08	0.267	2.51E-08	0.452	-1.01E-06	0.637	-6.75E-06
0.087	-6.67E-08	0.272	2.67E-08	0.457	-1.13E-06	0.642	-7.48E-06
0.092	-7.22E-08	0.277	2.90E-08	0.462	-1.26E-06	0.647	-8.28E-06
0.097	-6.83E-08	0.282	2.51E-08	0.467	-1.38E-06	0.652	-9.14E-06
0.102	-7.53E-08	0.287	2.20E-08	0.472	-1.51E-06	0.657	-1.01E-05
0.107	-6.83E-08	0.292	1.02E-08	0.477	-1.62E-06	0.662	-1.10E-05
0.112	-5.65E-08	0.297	3.92E-09	0.482	-1.73E-06	0.667	-1.21E-05
0.117	-4.87E-08	0.302	7.06E-09	0.487	-1.82E-06	0.672	-1.31E-05
0.122	-3.77E-08	0.307	6.28E-09	0.492	-1.90E-06	0.677	-1.42E-05
0.127	-2.90E-08	0.312	3.14E-09	0.497	-1.98E-06	0.682	-1.54E-05
0.132	-1.96E-08	0.317	-3.23E-13	0.502	-2.04E-06	0.687	-1.65E-05
0.137	-1.41E-08	0.322	-3.23E-13	0.507	-2.11E-06	0.692	-1.77E-05
0.142	-2.20E-08	0.327	-3.23E-13	0.512	-2.17E-06	0.697	-1.89E-05
0.147	-2.20E-08	0.332	-1.57E-08	0.517	-2.23E-06		
0.152	-2.20E-08	0.337	-2.67E-08	0.522	-2.26E-06		
0.157	-2.43E-08	0.342	-3.92E-08	0.527	-2.29E-06		
0.162	-1.33E-08	0.347	-4.47E-08	0.532	-2.32E-06		
0.167	-4.71E-09	0.352	-4.40E-08	0.537	-2.34E-06		
0.172	1.57E-09	0.357	-4.40E-08	0.542	-2.37E-06		
0.177	5.49E-09	0.362	-5.57E-08	0.547	-2.40E-06		
0.182	1.26E-08	0.367	-5.89E-08	0.552	-2.43E-06		

Table 9: ***Activity of nickel- indium composite at 7 deposition cycles using linear sweep voltammetry***

Potential/V	Current/A	Potential/V	Current/A	Potential/V	Current/A	Potential/V	Current/A
0.002	-2.47E-07	0.187	-1.85E-07	0.372	-5.63E-07	0.557	-4.23E-06
0.007	-2.60E-07	0.192	-1.85E-07	0.377	-6.13E-07	0.562	-4.40E-06
0.012	-2.68E-07	0.197	-1.85E-07	0.382	-7.10E-07	0.567	-4.63E-06
0.017	-2.70E-07	0.202	-1.93E-07	0.387	-1.05E-06	0.572	-4.93E-06
0.022	-2.72E-07	0.207	-1.95E-07	0.392	-2.38E-06	0.577	-5.33E-06
0.027	-2.64E-07	0.212	-1.99E-07	0.397	-3.76E-06	0.582	-5.84E-06
0.032	-2.56E-07	0.217	-2.01E-07	0.402	-4.39E-06	0.587	-6.46E-06
0.037	-2.55E-07	0.222	-2.07E-07	0.407	-5.05E-06	0.592	-7.25E-06
0.042	-2.54E-07	0.227	-2.07E-07	0.412	-5.28E-06	0.597	-8.24E-06
0.047	-2.48E-07	0.232	-2.12E-07	0.417	-5.25E-06	0.602	-9.43E-06
0.052	-2.50E-07	0.237	-2.10E-07	0.422	-5.13E-06	0.607	-1.09E-05
0.057	-2.48E-07	0.242	-2.25E-07	0.427	-4.93E-06	0.612	-1.26E-05
0.062	-2.46E-07	0.247	-2.21E-07	0.432	-4.66E-06	0.617	-1.46E-05
0.067	-2.48E-07	0.252	-2.28E-07	0.437	-4.38E-06	0.622	-1.70E-05
0.072	-2.45E-07	0.257	-2.35E-07	0.442	-4.12E-06	0.627	-1.96E-05
0.077	-2.27E-07	0.262	-2.40E-07	0.447	-3.89E-06	0.632	-2.26E-05
0.082	-2.26E-07	0.267	-2.48E-07	0.452	-3.70E-06	0.637	-2.60E-05
0.087	-2.24E-07	0.272	-2.52E-07	0.457	-3.55E-06	0.642	-2.96E-05
0.092	-2.18E-07	0.277	-2.58E-07	0.462	-3.46E-06	0.647	-3.35E-05
0.097	-2.14E-07	0.282	-2.67E-07	0.467	-3.42E-06	0.652	-3.77E-05
0.102	-2.18E-07	0.287	-2.72E-07	0.472	-3.40E-06	0.657	-4.21E-05
0.107	-2.09E-07	0.292	-2.87E-07	0.477	-3.41E-06	0.662	-4.68E-05
0.112	-2.01E-07	0.297	-2.96E-07	0.482	-3.43E-06	0.667	-5.16E-05
0.117	-2.03E-07	0.302	-3.05E-07	0.487	-3.47E-06	0.672	-5.66E-05
0.122	-2.04E-07	0.307	-3.19E-07	0.492	-3.51E-06	0.677	-6.17E-05
0.127	-1.99E-07	0.312	-3.34E-07	0.497	-3.55E-06	0.682	-6.69E-05
0.132	-1.94E-07	0.317	-3.46E-07	0.502	-3.60E-06	0.687	-7.21E-05
0.137	-1.93E-07	0.322	-3.58E-07	0.507	-3.64E-06	0.692	-7.73E-05
0.142	-1.92E-07	0.327	-3.66E-07	0.512	-3.68E-06	0.697	-8.24E-05
0.147	-1.83E-07	0.332	-3.81E-07	0.517	-3.71E-06		
0.152	-1.84E-07	0.337	-3.96E-07	0.522	-3.75E-06		
0.157	-1.82E-07	0.342	-4.11E-07	0.527	-3.79E-06		
0.162	-1.88E-07	0.347	-4.32E-07	0.532	-3.84E-06		
0.167	-1.87E-07	0.352	-4.52E-07	0.537	-3.88E-06		
0.172	-1.84E-07	0.357	-4.71E-07	0.542	-3.94E-06		
0.177	-1.92E-07	0.362	-4.90E-07	0.547	-4.01E-06		
0.182	-1.92E-07	0.367	-5.23E-07	0.552	-4.11E-06		

Table 10: ***Activity of nickel- gallium composite at 5 deposition cycles using linear sweep voltammetry***

Potential/V	Current/A	Potential/V	Current/A	Potential/V	Current/A	Potential/V	Current/A
0.002	2.23E-07	0.187	3.27E-07	0.372	1.75E-07	0.557	-5.41E-06
0.007	2.17E-07	0.192	3.27E-07	0.377	1.59E-07	0.562	-5.52E-06
0.012	2.10E-07	0.197	3.20E-07	0.382	1.47E-07	0.567	-5.62E-06
0.017	1.98E-07	0.202	3.13E-07	0.387	1.28E-07	0.572	-5.71E-06
0.022	1.95E-07	0.207	3.01E-07	0.392	9.97E-08	0.577	-5.83E-06
0.027	1.95E-07	0.212	3.17E-07	0.397	7.85E-08	0.582	-5.98E-06
0.032	2.01E-07	0.217	3.36E-07	0.402	5.10E-08	0.587	-6.18E-06
0.037	2.20E-07	0.222	3.39E-07	0.407	1.88E-08	0.592	-6.42E-06
0.042	2.35E-07	0.227	3.43E-07	0.412	-1.57E-08	0.597	-6.69E-06
0.047	2.39E-07	0.232	3.36E-07	0.417	-4.71E-08	0.602	-6.99E-06
0.052	2.37E-07	0.237	3.36E-07	0.422	-8.79E-08	0.607	-7.30E-06
0.057	2.32E-07	0.242	3.30E-07	0.427	-1.64E-07	0.612	-7.60E-06
0.062	2.24E-07	0.247	3.23E-07	0.432	-2.56E-07	0.617	-7.93E-06
0.067	2.26E-07	0.252	3.17E-07	0.437	-4.18E-07	0.622	-8.28E-06
0.072	2.25E-07	0.257	3.23E-07	0.442	-6.66E-07	0.627	-8.67E-06
0.077	2.43E-07	0.262	3.29E-07	0.447	-1.06E-06	0.632	-9.11E-06
0.082	2.57E-07	0.267	3.27E-07	0.452	-1.60E-06	0.637	-9.57E-06
0.087	2.71E-07	0.272	3.36E-07	0.457	-2.27E-06	0.642	-1.01E-05
0.092	2.74E-07	0.277	3.30E-07	0.462	-3.07E-06	0.647	-1.06E-05
0.097	2.70E-07	0.282	3.23E-07	0.467	-3.96E-06	0.652	-1.10E-05
0.102	2.68E-07	0.287	3.12E-07	0.472	-4.90E-06	0.657	-1.15E-05
0.107	2.67E-07	0.292	3.05E-07	0.477	-5.94E-06	0.662	-1.20E-05
0.112	2.71E-07	0.297	3.01E-07	0.482	-6.98E-06	0.667	-1.25E-05
0.117	2.73E-07	0.302	2.92E-07	0.487	-7.46E-06	0.672	-1.31E-05
0.122	2.81E-07	0.307	2.89E-07	0.492	-7.31E-06	0.677	-1.36E-05
0.127	2.93E-07	0.312	2.88E-07	0.497	-6.89E-06	0.682	-1.42E-05
0.132	3.07E-07	0.317	2.90E-07	0.502	-6.47E-06	0.687	-1.48E-05
0.137	3.05E-07	0.322	2.80E-07	0.507	-6.19E-06	0.692	-1.53E-05
0.142	2.97E-07	0.327	2.76E-07	0.512	-5.95E-06	0.697	-1.58E-05
0.147	3.03E-07	0.332	2.61E-07	0.517	-5.69E-06		
0.152	3.02E-07	0.337	2.54E-07	0.522	-5.47E-06		
0.157	2.98E-07	0.342	2.43E-07	0.527	-5.32E-06		
0.162	2.95E-07	0.347	2.28E-07	0.532	-5.23E-06		
0.167	3.10E-07	0.352	2.14E-07	0.537	-5.19E-06		
0.172	3.22E-07	0.357	2.02E-07	0.542	-5.21E-06		
0.177	3.32E-07	0.362	1.88E-07	0.547	-5.25E-06		
0.182	3.28E-07	0.367	1.81E-07	0.552	-5.31E-06		